



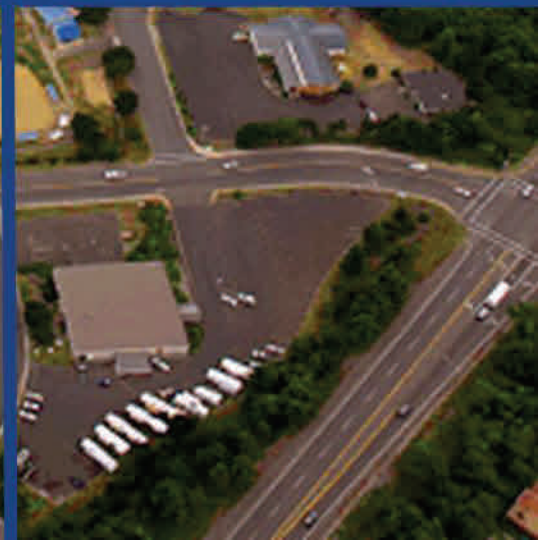
United States  
Environmental Protection  
Agency

EPA/600/R-10/128  
September 2010



# Approaches to Identify Exceedances of Water Quality Thresholds Associated with Ocean Conditions

# SCIENCE



Office of  
Research & Development

National Health and  
Environmental Effects  
Research Laboratory

# Approaches to Identify Exceedances of Water Quality Thresholds Associated with Ocean Conditions

Cheryl A. Brown and Walter G. Nelson  
National Health and Environmental Effects Research Laboratory  
Western Ecology Division  
Pacific Coastal Ecology Branch  
2111 SE Marine Science Dr.  
Newport, OR 97366





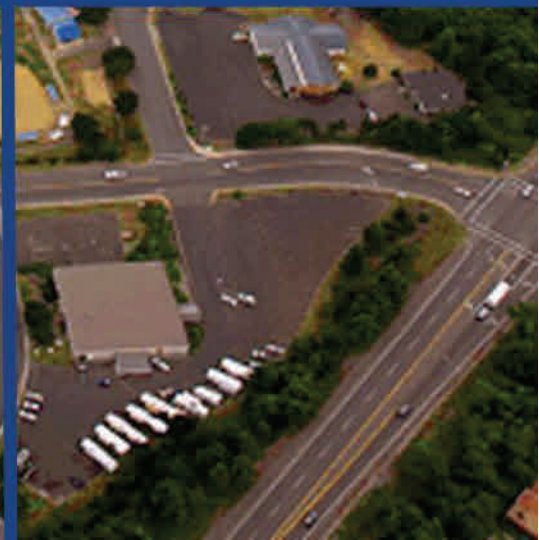
United States  
Environmental Protection  
Agency

EPA/600/R-10/128  
September 2010



## Approaches to Identify Exceedances of Water Quality Thresholds Associated with Ocean Conditions

# SCIENCE



Office of  
Research & Development

National Health and  
Environmental Effects  
Research Laboratory

**Abstract**

Estuaries along the west coast of the United States periodically have high nutrient, high chlorophyll *a*, and low dissolved oxygen levels due to the intrusion of oceanic water into the estuaries. This oceanic water often has water quality conditions which exceed water quality standards and indicators of eutrophication status. Tools are needed to distinguish such exceedances of water quality thresholds related to import of oceanic water from other causes. In this report, we present an application of logistic regression models to predict the probability of exceedance of water quality thresholds using flood-tide nutrient and dissolved oxygen data from the Yaquina Estuary. Models including water temperature and salinity correctly classified exceedances of dissolved inorganic nitrogen and phosphorous thresholds about 90% of the time, and for dissolved oxygen about 80% of the time. Inclusion of *in situ* fluorescence in the logistic regression model for dissolved oxygen improved the model performance and reduced the rate of false positives.

## Table of Contents

Abstract .....	2
List of Figures .....	4
List of Tables .....	5
Disclaimer .....	6
Acknowledgments.....	6
1. Introduction/Background .....	7
2. Methods.....	9
2.1 Data Used in the Analyses .....	9
2.1.1 Yaquina Estuary Flood-tide Nutrient Data .....	10
2.1.2 Yaquina Estuary Continuous Data.....	10
2.1.3 Additional Yaquina Estuary Data .....	11
2.1.4 Other Sources of Data.....	11
2.2 Data Analyses .....	12
2.2.1 Logistic Regression.....	13
3. Results and Discussion .....	14
3.1 Role of Oceanic Conditions in Causing Exceedances of Water Quality	
Thresholds.....	14
3.1.1 Nutrients.....	15
3.1.2 Dissolved Oxygen.....	17
3.2 Development of Indicators of Ocean Influence .....	18
3.2.1 Nutrients.....	18
3.2.2 Dissolved Oxygen.....	35
4. Summary .....	43
5. Literature Cited .....	49
Appendices.....	52

## List of Figures

Figure 1. Location map showing the location of flood-tide nutrient sampling and continuous monitoring station (Y1) inside Yaquina Estuary, and inner shelf stations from Wetz et al.....	9
Figure 2. Interannual variability in the percent of dry season observations with a) DIN > 14 $\mu\text{M}$ and b) DIP > 1.3 $\mu\text{M}$ in Zone 1. ....	16
Figure 3. Percent of dry season observations with DIN > 14 $\mu\text{M}$ in the lower estuary and median flood-tide water temperatures for each year.....	17
Figure 4. Percent of dry season observations of flood-tide dissolved oxygen < 6.5 $\text{mg l}^{-1}$ at station Y1 for each year. ....	18
Figure 5. DIN as a function of temperature and salinity generated using dry season data from a) the inner shelf off of Newport, Oregon and b) flood-tide samples from station Y1 in the Yaquina Estuary. ....	20
Figure 6. DIP as a function of temperature and salinity generated using dry season data from a) the inner shelf off of Newport, Oregon and b) flood-tide samples from station Y1 in the Yaquina Estuary. ....	21
Figure 7. False positive and false negative rates as a function of prediction point for the logistic regression model for DIN > 14 $\mu\text{M}$ using water temperature and salinity. ...	24
Figure 8. ROC curve for logistic regression model for DIN > 14 $\mu\text{M}$ using water temperature and salinity with an AUC value of 0.94.....	25
Figure 9. Temperature and salinity of cruise data measured in the Yaquina Estuary during the dry seasons of 1998-2008 with DIN $\leq$ 14 $\mu\text{M}$ and DIN > 14 $\mu\text{M}$ , and contours of probability of DIN > 14 $\mu\text{M}$ generated from logistic regression model with water temperature and salinity as explanatory variables. ....	28
Figure 10. Example of a mixing diagram showing a riverine DIN source. ....	29
Figure 11. Temperature and salinity of cruise data measured in the Yaquina Estuary during the dry seasons of 1998-2008 with DIP $\leq$ 1.3 $\mu\text{M}$ and DIP > 1.3 $\mu\text{M}$ , and contours of probability of DIP > 1.3 $\mu\text{M}$ generated from logistic regression model with water temperature and salinity as explanatory variables. ....	30
Figure 12. Flood-tide dissolved oxygen at station Y1 in the Yaquina Estuary plotted versus a) temperature and salinity, and b) sigma-t and <i>in situ</i> fluorescence.....	36
Figure 13. False positive and false negative rates as a function of prediction point for logistic regression model for dissolved oxygen < 6.5 $\text{mg l}^{-1}$ using water temperature and salinity as explanatory variables. ....	37
Figure 14. Temperature and salinity of cruise data measured in the Yaquina Estuary during May to October of 2006 and 2007 with DO $\geq$ 6.5 $\text{mg l}^{-1}$ and DO < 6.5 $\text{mg l}^{-1}$ , and contours of probability of DO < 6.5 $\text{mg l}^{-1}$ generated from logistic regression model with water temperature and salinity as explanatory variables. ....	41

## List of Tables

Table 1. Water quality thresholds used in development of logistic regression models. .....	<b>Error! Bookmark not defined.</b>
Table 2. Intercepts and coefficients for logistic regression models for exceedances of DIN and DIP thresholds.....	23
Table 3. Sample size and area under the receiver operating characteristic curve (AUC) for DIN and DIP models.....	24
Table 4. Classification table showing accuracy of the water temperature and salinity logistic regression equation at predicting DIN > 14 µM using the reserved data.....	26
Table 5. Classification table showing accuracy of the water temperature and salinity logistic regression equation at predicting DIP > 1.3 µM using the reserved data. ....	27
Table 6. Observed DIN and DIP, water temperature and salinity, and probability of exceeding nutrient thresholds calculated using water temperature and salinity at time of sampling and previous flood tide.....	33
Table 7. Observed median NO <sub>3</sub> <sup>-</sup> +NO <sub>2</sub> <sup>-</sup> and PO <sub>4</sub> <sup>-3</sup> for May – September 2008 and modeled using water temperature at time of sampling and water temperature during flood tide previous to sampling.....	34
Table 8. Intercepts and coefficients for logistic regression models for occurrences of dissolved oxygen <6.5 mg l <sup>-1</sup> .....	38
Table 9. Sample size and area under the receiver operating characteristic curve (AUC) for the dissolved oxygen models.....	38
Table 10. Classification table showing accuracy of the water temperature and salinity logistic regression equation for predicting the occurrence of flood-tide DO < 6.5 mg l <sup>-1</sup> using data collected during May – September 2009 at station Y1. ....	39
Table 11. Classification table showing accuracy of the water temperature, salinity, and <i>in situ</i> fluorescence logistic regression equation for predicting the occurrence of flood- tide DO < 6.5 mg l <sup>-1</sup> using data collected during May – September 2009 at station Y1. ....	40
Table A1. Classification table for DIN logistic regression with water temperature and salinity as explanatory variables for probability prediction points ranging from 0 to 1 .....	53
Table A2. Classification table for DIP logistic regression with water temperature and salinity as explanatory variables for probability prediction points ranging from 0 to 1 .....	54
Table A3. Classification table for dissolved oxygen logistic regression with water temperature and salinity as explanatory variables for probability prediction points ranging from 0 to 1 .....	55

**Disclaimer**

The information in this document has been funded wholly by the U.S. Environmental Protection Agency. It has been subjected to review by the National Health and Environmental Effects Research Laboratory and approved for publication. Approval does not signify that the contents reflect the views of the Agency, nor does mention of trade names or commercial products constitute endorsement or recommendation for use.

**Acknowledgments**

The authors would like to thank the following for their contributions to this report: Mr. T Chris Mochon Collura of Western Ecology Division (WED) for his work in calibration of the instruments; Dr. Robert Ozretich of WED for cruise data; Mr. Pat Clinton of WED for map production, Dr. Peter Eldridge (deceased) of WED for nutrient data; employees of Dynamac, Inc. for field work; and Dr. Melanie Frazier of WED for statistical advice and reviewing a previous version of this report.

## 1. Introduction/Background

In response to the Clean Water Act requirements to protect and restore the quality of surface waters of the nation, EPA has developed a strategy of assisting the States to develop numeric nutrient criteria as part of water quality standards designed to protect the designated uses of State waters. EPA has provided guidance to the States and Tribes for developing nutrient criteria for estuarine and coastal waters (US EPA, 2002). The Office of Research and Development, National Health and Environmental Effects Laboratory (NHEERL) has been conducting research to support improvements to the scientific basis for estuarine, numeric nutrient criteria. In the Pacific Northwest (PNW) region, NHEERL scientists have previously synthesized the research results of field sampling, trend analyses, and modeling approaches to produce a case study for development of numeric nutrient targets for Yaquina Estuary, Oregon (Brown et al., 2007).

Due to the seasonal variability in water quality conditions within the Yaquina Estuary, Brown et al. (2007) recommended that separate criteria be developed for wet (November – April) and dry seasons (May – October). Since there is little biological utilization of nutrients during the wet season, development of dry season criteria was suggested as a higher priority. In addition, it was recommended that the estuary be divided into two zones and separate criteria be developed for the ocean-dominated (Zone 1) and watershed and point source dominated (Zone 2) regions (see Figure 1). Using *in situ* observation within the Yaquina Estuary as a basis for determining an Estuarine Reference Condition, median values were suggested as potential dry season criteria for dissolved inorganic nitrogen (DIN) and phosphate. In the present report, the potential numeric criteria are termed “water quality thresholds.”

During April through September along the Pacific Northwest coast of the U.S., seasonal, wind-driven coastal upwelling advects relatively cool, nutrient rich water to the surface, which is then advected into the estuaries during flood tides. Previous studies have demonstrated that water quality conditions within PNW estuaries during the summer are influenced by intrusions of upwelled oceanic water into the estuaries, affecting nutrients (Haertel et al., 1969; de Angelis and Gordon, 1985; Brown and Ozretich, 2009), phytoplankton (Roegner and Shanks, 2001; Roegner et al., 2002; Brown and Ozretich, 2009), and dissolved oxygen (Pearson and Holt, 1960; Haertel et al., 1969;

Brown and Power, in review) levels. The coupling of water quality conditions between the coastal ocean and the adjacent estuaries can be problematic in assessing compliance of water quality standards and for evaluating eutrophication status for estuarine systems in the region.

The objective of this report is to provide a set of simple, statistical approaches that may be used to distinguish exceedances of water quality thresholds resulting from natural conditions in the near coastal ocean as distinct from other causes of exceedances. We used the physical characteristics of upwelled water, namely temperature and salinity, as indicators of upwelled water within the estuary. Statistical methods were then applied in order to develop a probability estimate that observations of water quality parameters such as nutrient or dissolved oxygen may have been strongly influenced by conditions in the near shore water and exceedances were associated with ocean conditions at time of sampling. An additional approach is presented where observed nutrient levels are compared to modeled values based on temperature-nutrient relationships developed using data from outside the estuary on the adjacent continental shelf.

## 2. Methods

### 2.1 Data Used in the Analyses

We assembled data primarily from a variety of research projects conducted by the Pacific Coastal Ecology Branch (U.S. EPA) to serve as the basis for development of statistical methods to detect the influence of near coast ocean waters on estuarine water quality conditions. EPA data were supplemented with additional data sources described below. Due to the multiple data sources, there is considerable interannual variability in sampling locations and sampling frequency. Although the studies used were not specifically designed to address issues of exceedances of water quality thresholds, they do allow us to examine the importance of variability of ocean conditions on water quality measurements within the estuary. All of the data used in the analyses was for the dry season, which is defined as the months of May through October.



Figure 1. Map showing the location of flood-tide nutrient sampling and continuous monitoring station (Y1) inside Yaquina Estuary, and inner continental shelf stations (NH-1 and NH-5) from Wetz et al. (2005). Meteorological data are available from NOAA station NWP03 and flood-tide water temperature data from station SBEO3. The boundary delineating Zone 1 and Zone 2 is also presented.

### 2.1.1 Yaquina Estuary Flood-tide Nutrient Data

During the period of May through October of 2002, 2003, and 2004, once daily water samples were collected during flood tides at an approximate depth of 0.5 m at the Oregon State University Dock (Y1, Figure 1), which is located inside Yaquina Estuary 4 km from the seaward end of the inlet jetties. Water samples were immediately filtered using GF/F filters and frozen for storage until analysis. Dissolved inorganic nutrients ( $\text{NO}_3^- + \text{NO}_2^-$ ,  $\text{NH}_4^+$ , and  $\text{PO}_4^{-3}$ ) were analyzed by MSI Analytical Laboratory (University of California-Santa Barbara, CA) using Lachat flow injection instrumentation (Zellweger Analytics, Milwaukee WI). Dissolved inorganic nitrogen (DIN) is composed of  $\text{NO}_3^-$ ,  $\text{NO}_2^-$ , and  $\text{NH}_4^+$ , and dissolved inorganic phosphorous (DIP) represents  $\text{PO}_4^{-3}$ . Commencing on August 28 2002 and continuing through September 2004, an automated sampler (ISCO<sup>®</sup>, Model 3700FR, Lincoln, NE, USA), programmed using the predicted time of each high tide, was used to collect water samples for each flood tide. Samples were held in a dark, refrigerated compartment and were collected daily, filtered and frozen for nutrient analysis.

### 2.1.2 Yaquina Estuary Continuous Data

During 2002-2009, time-series data (temperature, salinity and dissolved oxygen) were collected every 15 minutes at station Y1 in the Yaquina Estuary using water quality monitoring sondes (YSI 6600, YSI, Inc., Yellow Springs, OH, USA). Beginning in 2004, *in situ* fluorescence was also measured. The sondes were calibrated prior to use following the manufacturer's recommendations. Temperature sensors were factory calibrated by the manufacturer and their performance was checked prior to and subsequent to deployment. Conductivity was calibrated with a one-point calibration. The dissolved oxygen sensor was calibrated using the saturated air-in-water method. *In situ* fluorescence was calibrated with a two-point calibration, using reverse osmosis water and a rhodamine WT solution with data reported as  $\mu\text{g l}^{-1}$ . Sonde performance was checked in a flow-through seawater bath in the laboratory immediately before and after deployment. Several techniques were used to identify time periods of significant biological fouling of the sensors. These techniques included post-deployment calibration checks, comparison of results from adjacent stations, comparison to independent discrete measurements (if available), and comparison of the last few readings of a deployment to

the first few readings of the newly deployed sonde. If there was evidence of biofouling or sensor drift, these data were excluded from the analyses. Flood-tide values were identified and extracted from the 15-min data record using the maximum salinity data that occurred closest to the time of predicted high tides. During 2002-2004, two sondes were deployed at station Y1, one deployed about 1 m below the water surface and the second deployed about 2.5 m below the water surface. During 2007-2009, only one sonde was deployed at 2.5 m. Data from the 2.5- m depth sonde were utilized, with data from the 1-m depth sonde substituted to fill data gaps. During 2005 and 2006, there appeared to be a positive bias in salinity data; therefore, these data were excluded from analyses.

### **2.1.3 Additional Yaquina Estuary Data**

Additional data were collected by the Pacific Coastal Ecology Branch in Zone 1 of the Yaquina Estuary during the months of May through October of 1998-2008 either from water quality cruises or the OSU dock. Sampling stations extended from near the mouth to a distance of about 12 km up estuary. Data compiled included dissolved inorganic nutrients, dissolved oxygen, water temperature, and salinity. The data collected from 1998-2006 were previously described in Brown et al. (2007). During 2007, seven stations were sampled in the lower estuary approximately once per month from June 8<sup>th</sup> – September 25<sup>th</sup>. During May through October of 2007 and 2008, nutrient samples were collected approximately weekly at station Y1. This sampling was random with respect to tidal stage.

### **2.1.4 Other Sources of Data**

#### *Classification Dataset*

As part of a study to classify estuaries with regard to their susceptibility to nutrient enrichment (Lee and Brown, 2009), we have conducted short-term deployments of instruments to measure temperature, salinity and dissolved oxygen levels in several Oregon estuaries. Data sondes were deployed near the mouths of the Siletz (June 23-25, 2008), Tillamook (July 19-25, 2005), and Umpqua (June 21-26, 2005) estuaries during the summers of 2005 and 2008. Length of deployments varied from 2 to 7 days and the same calibration procedures described above were used for these deployments.

### *Coos Bay Dataset*

Continuous sonde data were also available for a station near the mouth of Coos Bay (Charleston Bridge Station at Latitude: 43° 20' 15.72" N, Longitude 124° 19' 13.92" W) from the South Slough National Estuarine Research Reserve (<http://nerrs.noaa.gov/SouthSlough/>).

### *Nearshore Data*

Additionally, we compared the flood-tide data collected at station Y1 to temperature, salinity and nutrient data from 1997 through 2004 that were available from Wetz et al. (2005) for two stations on the inner continental shelf off Newport, Oregon (NH-5, NH-15, Figure 1). Data from the months of May through October, which coincides with the period during which upwelling predominantly occurs, were extracted. Hourly wind speed and direction data were available from a near shore NOAA weather station adjacent to the Yaquina Estuary (NWP03, Figure 1; <http://www.ndbc.noaa.gov/>). Flood-tide nutrient, water temperature, and dissolved oxygen conditions at station Y1 have previously been correlated with integrated alongshore wind stress (Brown and Ozretich, 2009; Brown and Power, in review). Integrated alongshore wind stress (with a decay coefficient of 2 days) was calculated using wind data from station NWP03 during the years of 1998-2008. Details on calculation of integrated alongshore wind stress are provided in Brown and Ozretich (2009). In this report, a positive wind stress indicates upwelling favorable wind stress from the north. Water temperature data were available from a NOAA station located inside the Yaquina Estuary (SBEO3, Figure 1; [http://www.ndbc.noaa.gov/station\\_page.php?station=sbeo3](http://www.ndbc.noaa.gov/station_page.php?station=sbeo3)).

## **2.2 Data Analyses**

The first step in identifying exceedances of water quality thresholds associated with ocean input is to specify the target thresholds (Table 1). Potential numeric targets for DIN and DIP have been previously identified by Brown et al. (2007). These thresholds are based on dry season median values of DIN and DIP for Zone 1 in the Yaquina Estuary. The threshold for dissolved oxygen is the state of Oregon criterion for estuarine waters ([http://arcweb.sos.state.or.us/rules/OARs\\_300/OAR\\_340/340\\_041.html](http://arcweb.sos.state.or.us/rules/OARs_300/OAR_340/340_041.html)).

Parameter	Threshold	Source
DIN	14 $\mu\text{M}$	Brown et al. (2007)
DIP	1.3 $\mu\text{M}$	Brown et al. (2007)
Dissolved Oxygen	6.5 $\text{mg l}^{-1}$	State of Oregon Criterion for Estuaries

### 2.2.1 Logistic Regression

To develop indicators that can be used to determine whether ocean conditions are responsible for exceedances of water quality thresholds, we used logistic regression models. Logistic models can be used to predict the probability of an event when the dependent variable is dichotomous. Logistic regression models have the form of

$$\text{logit}(p) = \beta_0 + \sum_{j=1}^k \beta_j x_j \quad (\text{Eq. 1})$$

where in our application  $p$  is the probability of exceedance of a water quality threshold and  $\beta_0$  is a constant,  $\beta_1, \beta_2, \dots, \beta_k$  are the regression coefficients of variables  $x_1, x_2, \dots, x_k$ , respectively. The probability of an event occurring can be calculated as

$$p = \frac{1}{1 + e^{-\text{logit}(p)}} \quad (\text{Eq. 2})$$

The logistic regression models were used to predict the probabilities that water quality thresholds were exceeded due to ocean conditions at the time of sampling. Logistic regression equations were generated for DIN, DIP, and dissolved oxygen water quality thresholds (Table 1). To create a dichotomous outcome for each dependent variable, a threshold value which is indicative of a potential water quality objective or threshold was specified. For DIN and DIP, if nutrient levels exceeded the threshold of either 14  $\mu\text{M}$  or 1.3  $\mu\text{M}$ , respectively, then a value of 1 was assigned (i.e., water quality objective not met), otherwise it was assigned a value of 0. For dissolved oxygen, if concentrations were below the threshold of 6.5  $\text{mg l}^{-1}$ , a value of 1 was assigned; otherwise it was assigned a 0. All logistic regression models were generated using R (version 2.8.1; R Development Core Team, 2008).

Logistic regression models were generated using the following explanatory variables: 1) water temperature, 2) water temperature and salinity, and 3) sigma-t (calculated from water temperature and salinity). For dissolved oxygen, an additional logistic regression model was developed using water temperature, salinity, and *in situ* fluorescence as explanatory variables. All models were developed using flood-tide data, since this is representative of oceanic water advected into the estuary.

To validate the logistic regression models, we randomly selected 20% (108 data points) of the 2002-2004 flood-tide nutrient data and reserved it for model validation. These reserved observations were randomly selected for DIN and DIP independently. For the dissolved oxygen logistic regression model, we used flood-tide dissolved oxygen data collected at station Y1 in May to September 2009 for model validation. Since water temperature and salinity were not measured at the time of nutrient sample collection, we used the continuous data described in the previous section for these parameters.

### **3. Results and Discussion**

#### **3.1 Role of Oceanic Conditions in Causing Exceedances of Water Quality Thresholds**

Numerous studies have found that there is considerable interannual variability in oceanic conditions on the shelf in the California Current Region resulting in variability in nutrient, chlorophyll *a*, and dissolved oxygen levels (Corwith and Wheeler, 2002; Thomas et al., 2003; Wheeler et al., 2003; Grantham et al., 2004; Barth et al., 2007). In addition, it has been demonstrated that conditions on the shelf influence water quality conditions within PNW estuaries (Roegner and Shanks, 2001; Roegner et al., 2002; Brown and Ozretich, 2009). Upwelling conditions typically result in high concentrations of DIN and DIP and lower concentrations of dissolved oxygen in surface waters that get advected into PNW estuaries. The magnitudes of increased nutrient or decreased oxygen concentrations vary with the year- to-year strength of upwelling. Therefore, it follows that non-attainments of estuarine water quality criteria may be related to interannual variability in ocean conditions.

### 3.1.1 Nutrients

To examine the importance of interannual variability in ocean conditions on nutrient levels within the estuary, we used the lower estuary (Zone 1) dry season nutrient threshold values presented in Table 1. We then calculated the number of exceedances of these thresholds for each year over the period 1998-2008 based on nutrient-cruise data. It is important to note that the data used to examine interannual variability in exceedances includes the data used to generate the criteria for the years of 1998-2006. The 90% confidence intervals for the percent of observations constituting exceedances of the nutrient thresholds were calculated following the method of Donohue and van Looij (2001). An annual exceedance of the nutrient threshold is determined if the lower 90% confidence interval falls above the level of 50% of observations as exceedances.

Based on this technique, the criterion for DIN (based on median values) would be exceeded during 2001 and 2002 (Figure 2a) and the DIP criterion would be exceeded in 2002 (Figure 2b). For an additional comparison, we used the flood-tide nutrient samples collected as the OSU dock in 2002, 2003, and 2004. The percent of observations exceeding the DIN threshold was similar to that for the cruise data in each year (Figure 2a). There was a significant correlation between the annual percent of observations exceeding the DIN and DIP thresholds ( $r = 0.87$ ,  $p = 0.001$ , Pearson Product Moment Correlation), because the ocean is the primary source of both of these nutrients in the lower estuary.

In the dry season, there is also a significant correlation between interannual variability in exceedances and median flood-tide water temperature (Figure 3), which is an indicator of the relative strength of coastal upwelling (Brown and Ozretich, 2009). The rate of exceedances of the DIN threshold was lowest in 1998, concurrent with El Niño conditions on the Oregon shelf, and an associated reduction in coastal upwelling. El Niño conditions occurred on the Oregon shelf from August 1997 through July 1998, and as a result, nutrient conditions were low on the inner shelf (Peterson et al., 2002). The highest rate of exceedances of the DIN threshold occurred in 2002, which coincided with anomalous conditions on the Oregon shelf. There was an intrusion of a subarctic water mass (Kosro, 2003) onto the Oregon shelf, and as a result the shelf water was cooler than usual and had higher than normal nutrient levels (Wheeler et al., 2003).

Interestingly, the rate of exceedances is not correlated with the Bakun upwelling index (daily values for latitude 45 °N, longitude 125°W averaged over the interval of May to October for each year). Menge et al. (2009) suggested that the Bakun index does not adequately reflect the magnitude of upwelling conditions occurring in the nearshore region.

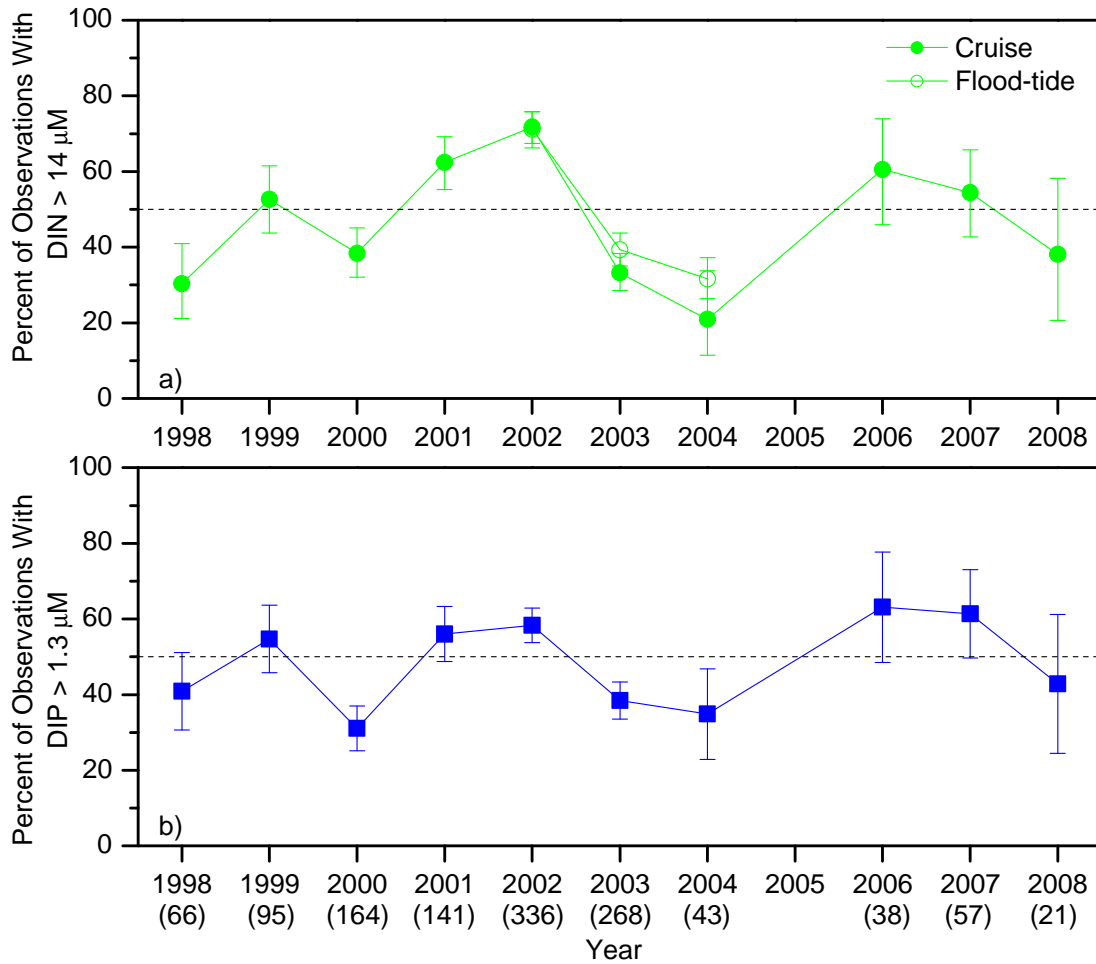


Figure 2. Interannual variability in the percent of dry season observations with a)  $\text{DIN} > 14 \mu\text{M}$  (filled symbols are cruise data and open symbols are flood-tide OSU dock samples) and b)  $\text{DIP} > 1.3 \mu\text{M}$  in Zone 1. The sample size of the cruise data is presented in parentheses below each year in panel b. The error bars represent 90% confidence intervals.

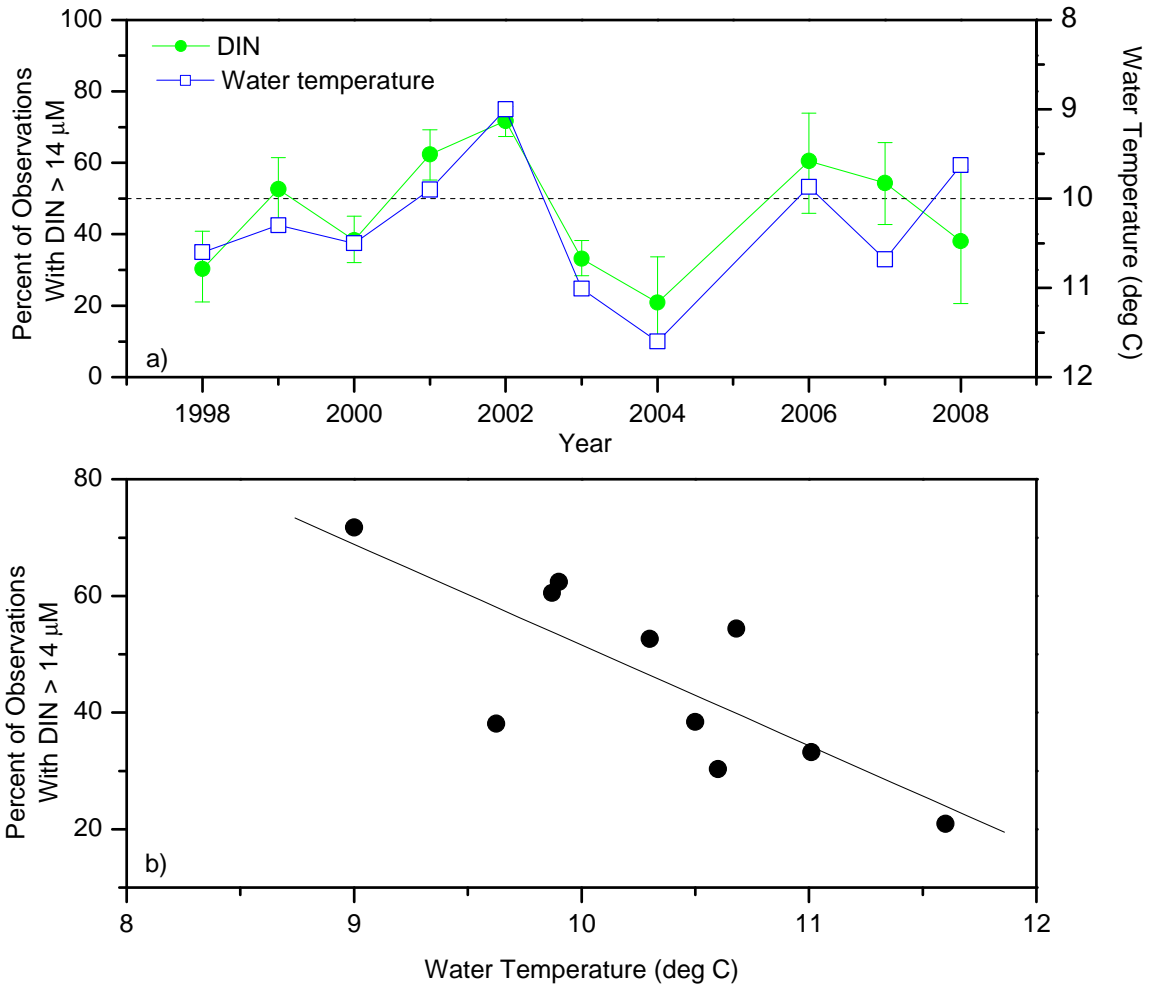


Figure 3. a) Percent of dry season observations with DIN > 14  $\mu\text{M}$  in the lower estuary and median flood-tide water temperatures for each year. b) Linear regression of the two variables (Percent observations exceeding threshold =  $224.3 - 17.27 * \text{water temperature}$ ,  $r^2 = 0.61$ ,  $p < 0.01$ ). Median water temperatures were calculated using flood-tide values from station Y1 for 2001 and 2003-2008, other years were calculated using water temperature data from SBEO3.

### 3.1.2 Dissolved Oxygen

There is considerable interannual variability in the percent of flood-tide observations with dissolved oxygen levels less than  $6.5 \text{ mg l}^{-1}$  at station Y1 (Figure 4a). During 2006, 56% of the flood tides had dissolved oxygen  $< 6.5 \text{ mg l}^{-1}$ , which coincided with strong upwelling conditions near Newport, Oregon. The lowest percentage occurrence of dissolved oxygen  $< 6.5 \text{ mg l}^{-1}$  occurred in 2005. There was a delay in the onset of upwelling on the Oregon coast during 2005 (Barth et al., 2007). Previously, we have demonstrated that there is a significant correlation between integrated alongshore

wind stress and flood-tide dissolved oxygen values in the Yaquina Estuary (Brown and Power, in review). Figure 4b shows that there is also a significant correlation between percent of flood-tide observations with dissolved oxygen below the criterion and median, integrated alongshore wind stress for May through October ( $p < 0.05$ ).

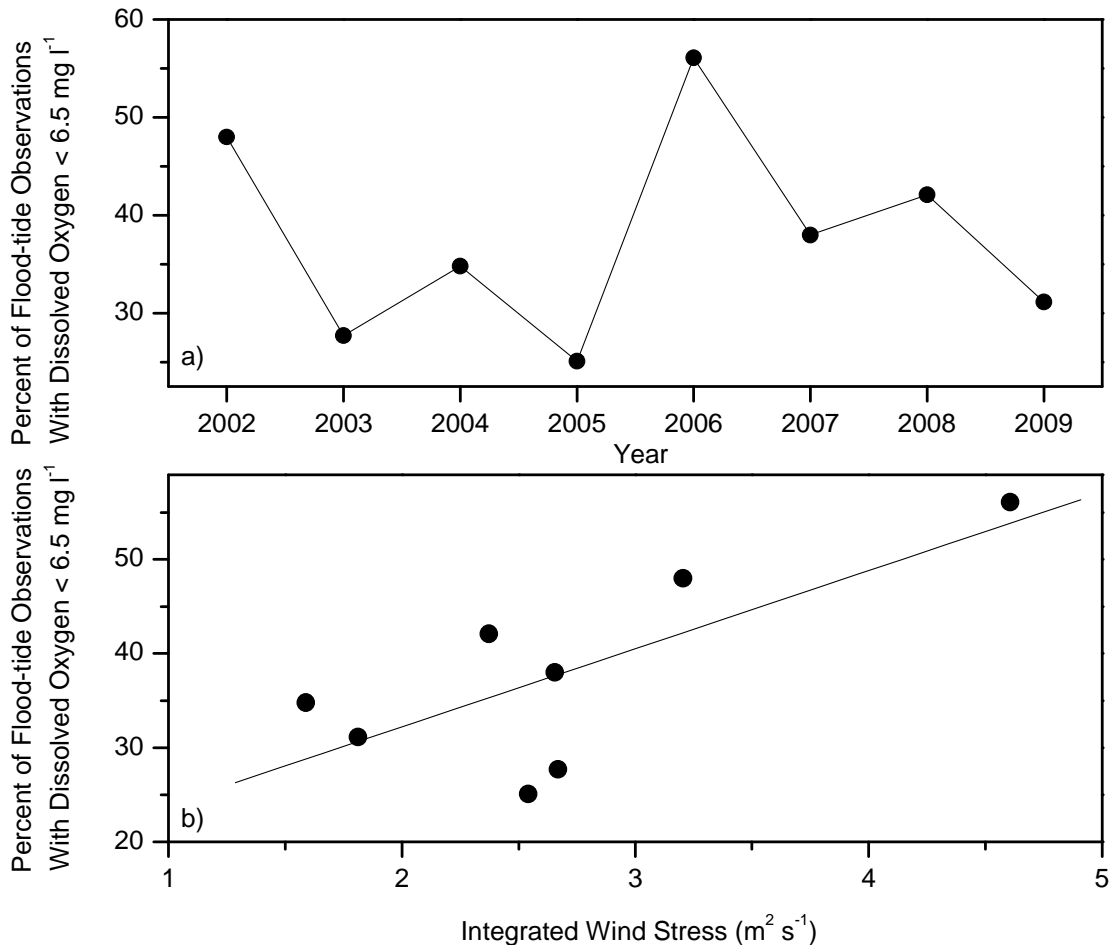


Figure 4. a) Percent of dry season observations of flood-tide dissolved oxygen  $< 6.5 \text{ mg l}^{-1}$  at station Y1 for each year. b) Linear regression of exceedances versus median integrated wind stress at station NWP03, with positive values indicating upwelling conditions. Years with the highest percentage occurrence of dissolved oxygen  $< 6.5 \text{ mg l}^{-1}$  coincide with strong upwelling conditions (Percent observations exceeding threshold =  $15.59 - 8.308 * \text{wind stress}$ ,  $r^2 = 0.54$ ,  $p < 0.05$ ).

### 3.2 Development of Indicators of Ocean Influence

#### 3.2.1 Nutrients

In the previous section, it was shown that ocean conditions can influence water quality conditions within the Yaquina Estuary. Consequently, it is desirable to develop indicators which will allow us to distinguish exceedances of water quality thresholds that

are related to ocean conditions from other causes. Previously, we have demonstrated that flood-tide water temperatures are strongly correlated with inner shelf water temperature (Brown and Power, in review) and alongshore wind stress (Brown and Ozretich, 2009). In addition, Nelson and Brown (2008) demonstrated that nitrate and phosphate levels in flood-tide water samples collected in the Yaquina Estuary can be modeled using flood-tide water temperatures. Figures 5 and 6 show DIN and DIP as a function of water temperature and salinity generated using either data from the inner shelf or flood-tide samples from the Yaquina Estuary. Water density ( $\sigma_t$  values) contours are also presented. High DIN and DIP concentrations occur at high salinities ( $>33$  psu), cold water temperatures ( $< 10$  °C), and high water densities ( $\sigma_t > 26$  kg m<sup>-3</sup>) both on the shelf and within the estuary. Peak DIN and DIP concentrations associated with coastal upwelling in the PNW are equivalent to concentrations defined as representing medium and high categories of eutrophication status when DIN and DIP are used as water quality indicators (Bricker et al., 2003). The DIN and DIP thresholds presented in Table 1 are exceeded in 45% and 48% of the flood-tide observations at station Y1 (Figures 5b and 6b), respectively.

### *Logistic Regression*

We used the flood-tide DIN and DIP data (Figure 5) to generate logistic regression models, which can be used to predict the probability of DIN and DIP exceeding the thresholds of 14  $\mu$ M and 1.3  $\mu$ M, respectively. Logistic regression models were generated for three sets of explanatory variables: 1) water temperature, 2) water temperature and salinity, and 3) water density ( $\sigma_t$ ).

The intercepts and coefficients (including standard errors and p-values) of each of the logistic regression models generated for DIN and DIP are presented in Table 2. To use a logistic regression model to predict the probability of an occurrence of an event being modeled, the user needs to specify the prediction point. If the modeled probability exceeds the prediction point, then the model predicts that the event being modeled has occurred (in this case the nutrient threshold has been exceeded). The selection of the prediction point represents a trade off between type I (false positive) and type II (false negative) errors. Examples of classification tables for the DIN and DIP logistic

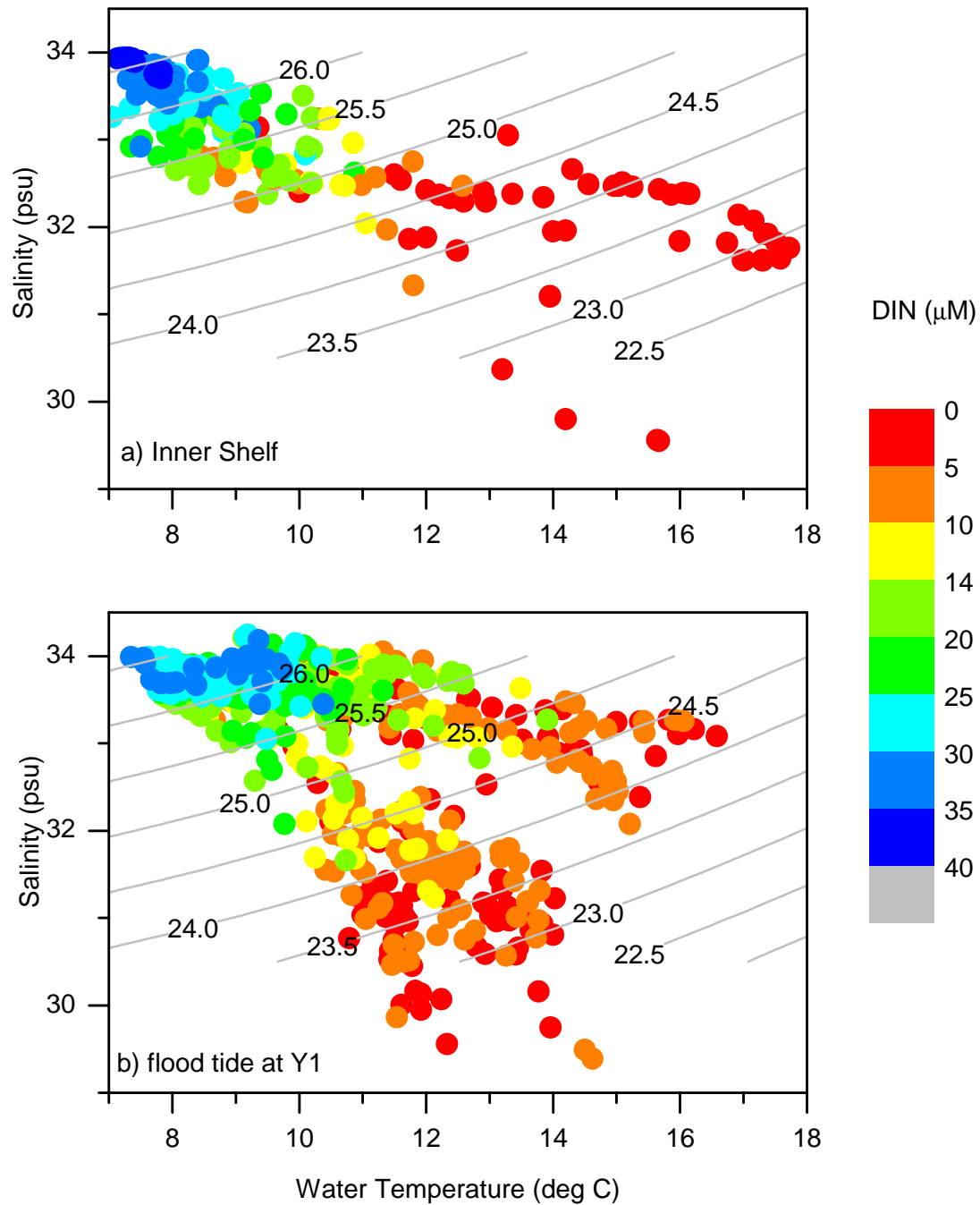


Figure 5. DIN as a function of temperature and salinity generated using dry season data from a) the inner shelf off of Newport, Oregon (Stations NH-5 and NH-15 from Wetz et al., 2005) and b) flood-tide samples from station Y1 in the Yaquina Estuary. The color of the symbol indicates DIN concentration ( $\mu\text{M}$ ) and the contours indicate sigma-t values.

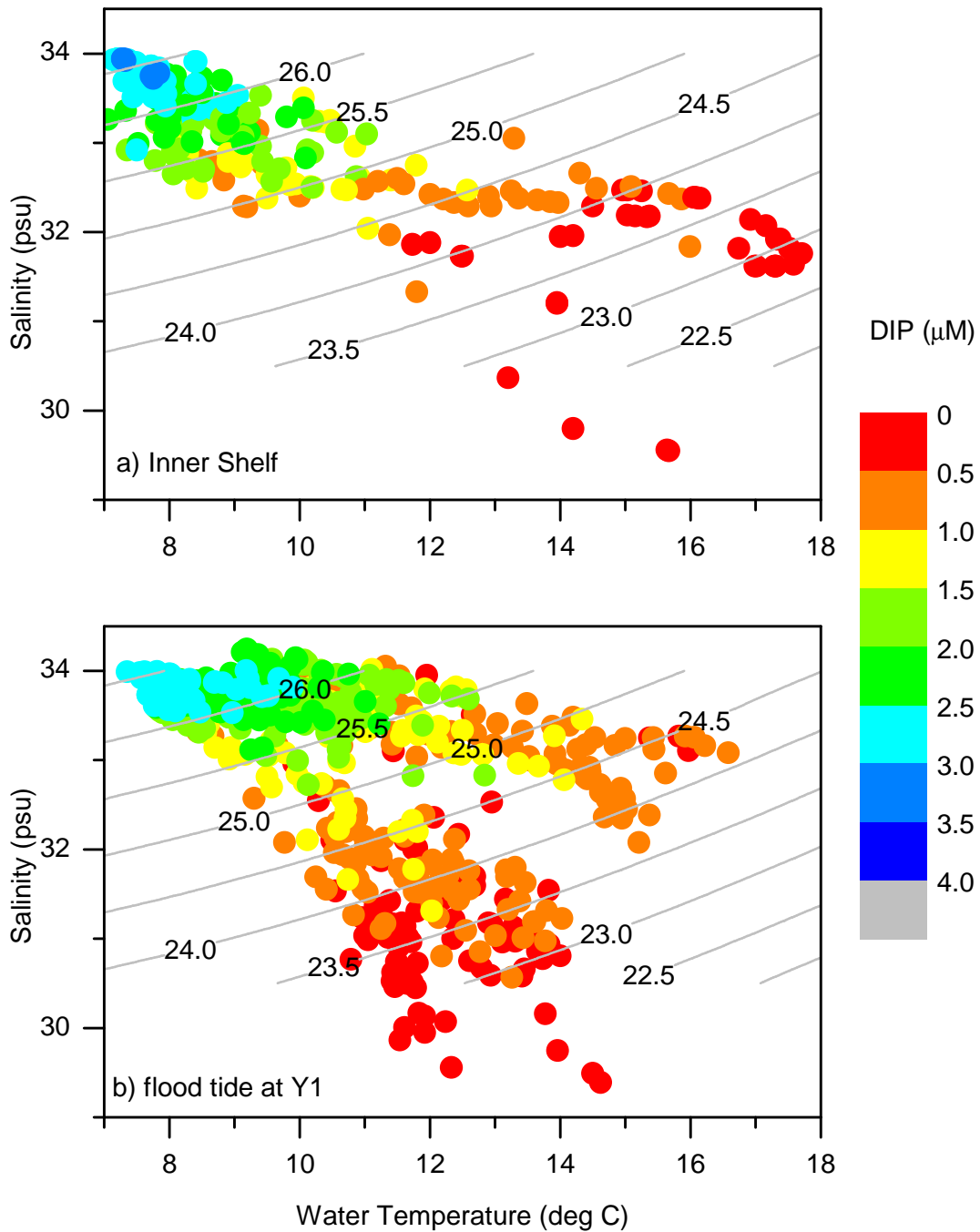


Figure 6. DIP as a function of temperature and salinity generated using dry season data from a) the inner shelf off of Newport, Oregon (Stations NH-5 and NH-15 from Wetz et al., 2005) and b) flood-tide samples from station Y1 in the Yaquina Estuary. The color of the symbol indicates DIP concentration ( $\mu\text{M}$ ) and the contours indicate sigma-t values.

regression models using water temperature and salinity as explanatory variables are presented in Tables A1 and A2. These classification tables show the number of observations correctly and incorrectly classified as exceeding the DIN and DIP thresholds as a function of prediction point generated with the data used to create the models.

A false positive is when the logistic model predicts that the nutrient threshold will be exceeded but the observed value does not exceed the threshold. A false negative is when the logistic model predicts that the threshold will not be exceeded, but the observed value exceeds the threshold. The false positive rate is the total number of false positives divided by the number of observations below the threshold. The false negative rate is the total number of false negatives divided by the number of observations that exceed the threshold. Selection of a lower prediction point (i.e., lowering the probability threshold that needs to be exceeded) results in an increase in sensitivity (number of times the model correctly predicts an exceedance of the threshold compared to the total number of observations that exceed the threshold) at the cost of increasing the occurrence of false positives. To evaluate the optimal prediction point, the false positive and false negative rates are plotted versus prediction point (Figure 7). The optimal prediction point is where the false positive and false negative rates are equal (or the intersection of the two curves). The optimal prediction points for each of the nutrient models are presented in Table 3.

The logistic regression models can be used to develop cutpoints for identification of exceedances associated with ocean input. Development of such cutpoints would allow users to simply compare their observed temperature or density to these values to discern whether exceedances are related to ocean input. Combining the optimal prediction points and the equations for the logistic regression using only water temperature as the explanatory variable results in a water temperature cutpoint for DIN and DIP exceedances of 10.6 °C. Thus, these logistic regression models predict that exceedances of DIN and DIP thresholds are related to ocean input when the water temperature is less than 10.6 °C. The water density cutpoints for DIN and DIP exceedances are sigma-t values of 25.67 and 25.59 kg m<sup>-3</sup>, respectively (see Figures 5 and 6).

Receiver operating characteristic (ROC) curves are often used to evaluate the predictive capabilities of models (Figure 8). ROC curves are generated by plotting true positive rate or sensitivity (ratio of the number of times the model correctly predicts an

exceedance of the threshold compared to the total number of observations that exceed the threshold) versus false positive rate (ratio of the number of times the model incorrectly predicts an exceedance of the threshold compared to the total number of observations less than the threshold) for prediction points ranging from 0 to 1. The values plotted in ROC curves are expressed as ratios rather than the percentages presented in the Appendix tables. An example of an ROC curve for the DIN > 14  $\mu$ M model using water temperature and salinity as explanatory variables is presented in Figure 8.

Table 2. Intercepts and coefficients for logistic regression models for exceedances of DIN and DIP thresholds			
	<b>Parameter</b>	<b>Standard error</b>	<b>p value</b>
<b>DIN using water temperature</b>			
Intercept	14.729	1.390	p < 0.001
Water temperature	-1.417	0.133	p < 0.001
<b>DIN using water temperature and salinity</b>			
Intercept	-56.5829	11.4365	p < 0.001
Water temperature	-0.9373	0.1345	p < 0.001
Salinity	1.9937	0.3333	p < 0.001
<b>DIN using sigma-t</b>			
Intercept	-88.9207	9.3790	p < 0.001
Sigma-t	3.4799	0.3648	p < 0.001
<b>DIP using water temperature</b>			
Intercept	14.4256	1.3796	p < 0.001
Water temperature	-1.3656	0.1306	p < 0.001
<b>DIP using water temperature and salinity</b>			
Intercept	-91.6108	14.8188	p < 0.001
Water temperature	-0.8167	0.1333	p < 0.001
Salinity	3.0139	0.4374	p < 0.001
<b>DIP using sigma-t</b>			
Intercept	-106.5114	11.1929	p < 0.001
Sigma-t	4.1778	0.4362	p < 0.001

Table 3. Sample size and area under the receiver operating characteristic curve (AUC) for DIN and DIP models. The optimal prediction points (false negative = false positive rates) are presented for each model.			
Model	N	AUC	Optimal Prediction Point
DIN using water temperature	431	0.91	0.45
DIN using water temperature and salinity	431	0.94	0.55
DIN using sigma-t	431	0.94	0.55
DIP using water temperature	431	0.90	0.49
DIP using water temperature and salinity	431	0.96	0.60
DIP using sigma-t	431	0.96	0.60

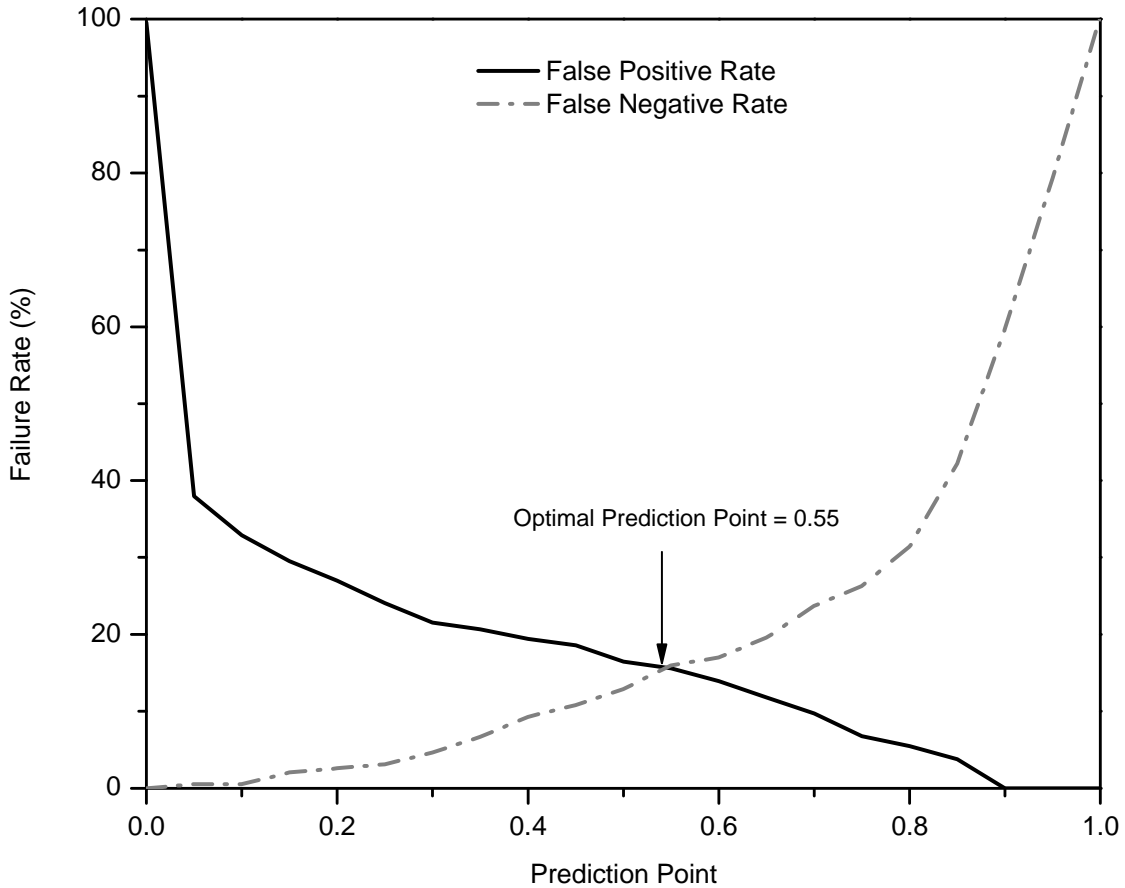


Figure 7. False positive and false negative rates as a function of prediction point for the logistic regression model for DIN > 14  $\mu$ M using water temperature and salinity. Optimal prediction point (0.55) is where overall failure rate is minimized and is located at the intersection of the two curves.

Models with high predictive capacity have curves that rise rapidly and have larger areas under the curve (AUC). An ideal model would have an AUC value of 1. Hosmer and Lemeshow (2000) suggest that if the area under the ROC curve is  $\geq 0.9$  the model has ‘outstanding’ discrimination; for AUC values between 0.8 and 0.9, the model has ‘excellent’ discrimination capability; for AUC values between 0.7 and 0.8, the model has ‘acceptable’ discrimination; and if the AUC = 0.5, the model has no discrimination capability. All of the models computed for the nutrient thresholds had ‘outstanding’ discrimination capability (Table 3); however, the models which included salinity consistently had higher AUC values than those models which omitted salinity.

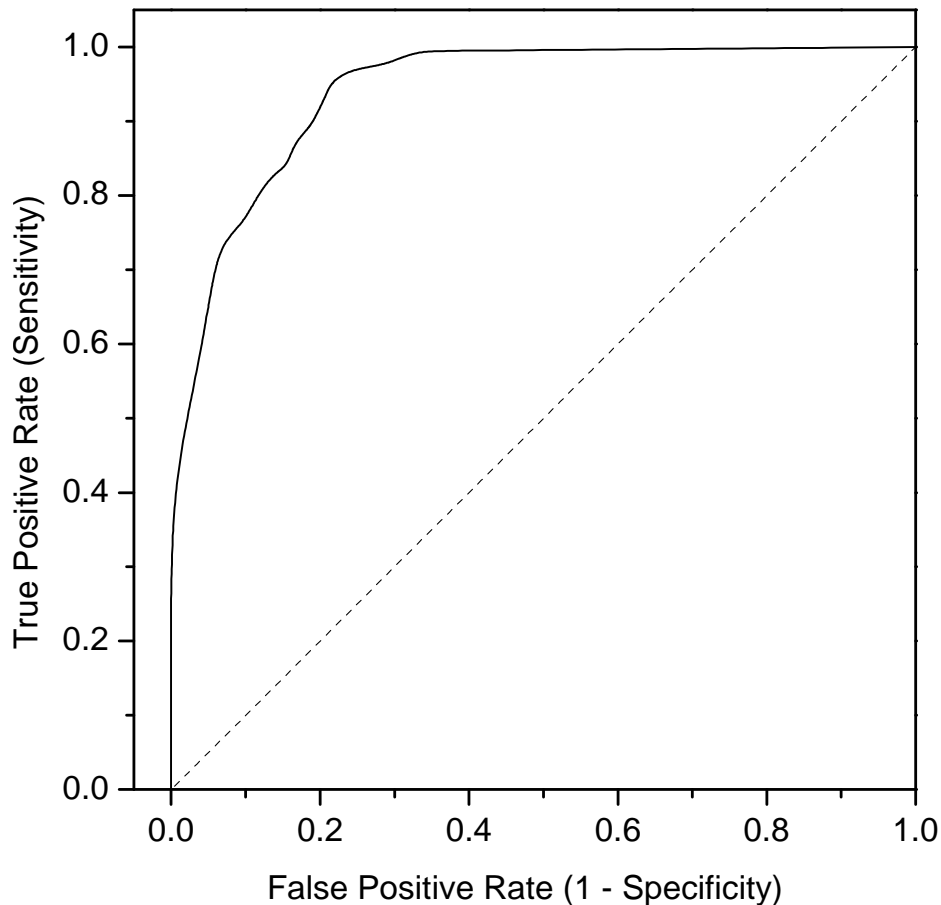


Figure 8. ROC curve for logistic regression model for  $\text{DIN} > 14 \mu\text{M}$  using water temperature and salinity with an AUC value of 0.94. The dashed line indicates the line of no discrimination capability (i.e., random guess).

### *Model Validation*

The predictive capability of the models was tested using the data which were reserved for model validation. For model validation, we used the models with water temperature and salinity as explanatory variables which had the highest AUC values and used the optimal prediction points of 0.55 and 0.60 for DIN and DIP, respectively. For each observation, the probability of exceeding the threshold was predicted using the logistic regression model, and if the probability was greater than the optimal prediction point, then the observation was predicted to exceed the threshold. Because the data used to generate the logistic regression models were exclusively flood-tide values, then a modeled exceedance of a water quality threshold represents the effect of ocean conditions at the time of sampling.

Prediction accuracies of the models for the reserved data are presented in 2x2 classification tables (Tables 4 and 5). The logistic regression models had an overall accuracy of 88.9% and 90% for DIN and DIP, respectively. Sensitivity is ratio of the number of times the model correctly predicts an exceedance to total number of observed exceedances. Specificity is defined as the ratio of correctly classified occurrences of nutrients less than the threshold to total number of observed occurrences less than the threshold. The sensitivity of the models was 89.8% and 89.3% for DIN and DIP, respectively. The specificity of the models was 88.1% and 92.3% for DIN and DIP, respectively.

	Predicted Occurrence of DIN		Total
	$\leq 14 \mu\text{M}$	$> 14 \mu\text{M}$	
Observed DIN $\leq 14 \mu\text{M}$	52	7	59
Observed DIN $> 14 \mu\text{M}$	5	44	49
Total	57	51	108

Table 5. Classification table showing accuracy of the water temperature and salinity logistic regression equation for predicting the occurrence of DIP > 1.3 $\mu\text{M}$ using the reserved data. Prediction point = 0.60.			
	Predicted Occurrence of DIP		Total
	$\leq 1.3 \mu\text{M}$	$> 1.3 \mu\text{M}$	
Observed DIP $\leq 1.3 \mu\text{M}$	48	4	52
Observed DIP $> 1.3 \mu\text{M}$	6	50	56
Total	54	54	108

*Demonstration of Application of Logistic Regression Model*

We applied the logistic regression models for DIN and DIP to water temperature and salinity data collected concurrently with nutrient data during the dry seasons of 1998-2008 in the marine-dominated portion (Zone 1) of the Yaquina Estuary. The temperature and salinity of DIN observations that either exceeded the 14  $\mu\text{M}$  threshold (filled circles) or fell below the threshold (open circles), together with the probability contours of the logistic regression model are presented in Figure 9. Fifty percent of the DIN observations exceeded the 14  $\mu\text{M}$  threshold, which is to be expected since it was based on the median value of dry season data from 1998-2006. The logistic regression model predicts that 46% of the DIN exceedances of the 14  $\mu\text{M}$  threshold are associated with ocean input (these data points are indicated with a green “x” in Figure 9). There is also evidence of a riverine DIN source, which the logistic regression model does not identify as ocean input. We, therefore, examined mixing diagrams (i.e., salinity versus DIN graphs) to identify observations where the exceedance of the DIN threshold can be attributed to a riverine source (red “x”, Figure 9). Figure 10 shows an example of a mixing diagram which indicates a riverine source for DIN.

The temperature and salinity of DIP observations that either exceeded the 1.3  $\mu\text{M}$  threshold (filled circles) or fell below the threshold (open circles), together with the probability contours of the logistic regression model are presented in Figure 11. Forty seven percent of the DIP observations exceeded the 1.3  $\mu\text{M}$  threshold and the model predicts that 44% of these exceedances are associated with ocean input (indicated by a green “x” in Figure 11). There are fewer observations exceeding the DIP threshold at relatively low salinities (< 27 psu), than there are for the DIN observations, this is

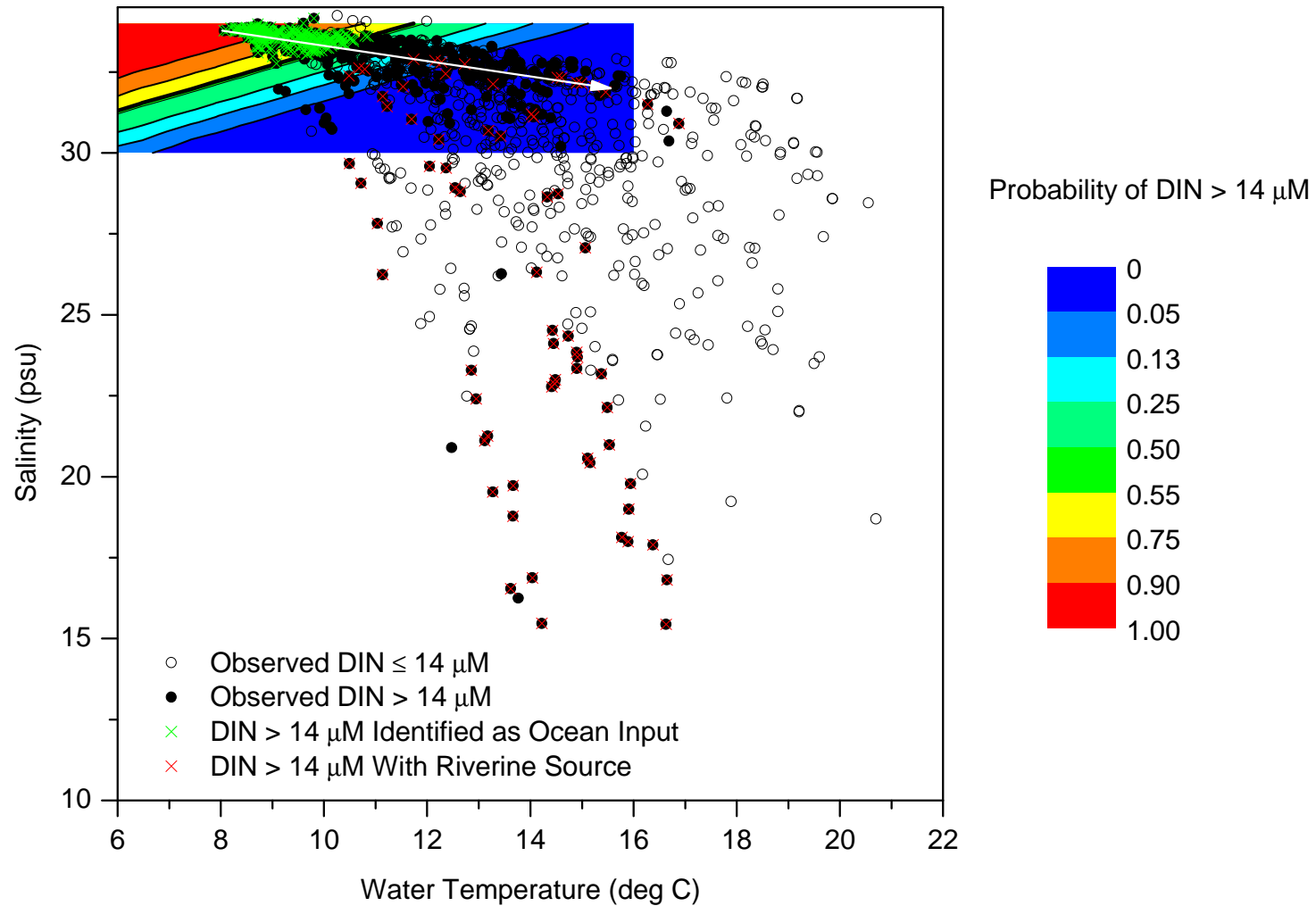


Figure 9. Temperature and salinity of cruise data measured in the Yaquina Estuary during the dry seasons of 1998-2008 with  $\text{DIN} \leq 14 \mu\text{M}$  (open circles) and  $\text{DIN} > 14 \mu\text{M}$  (filled circles), and contours of probability of  $\text{DIN} > 14 \mu\text{M}$  generated from logistic regression model with water temperature and salinity as explanatory variables. The green “x” symbols are observations of  $\text{DIN} > 14 \mu\text{M}$  identified as ocean input from the logistic regression model with a prediction point of 0.55 the red “x” symbols are those that appear to have a riverine DIN source, as determined from mixing diagrams. The white arrow indicates a heating and mixing line.

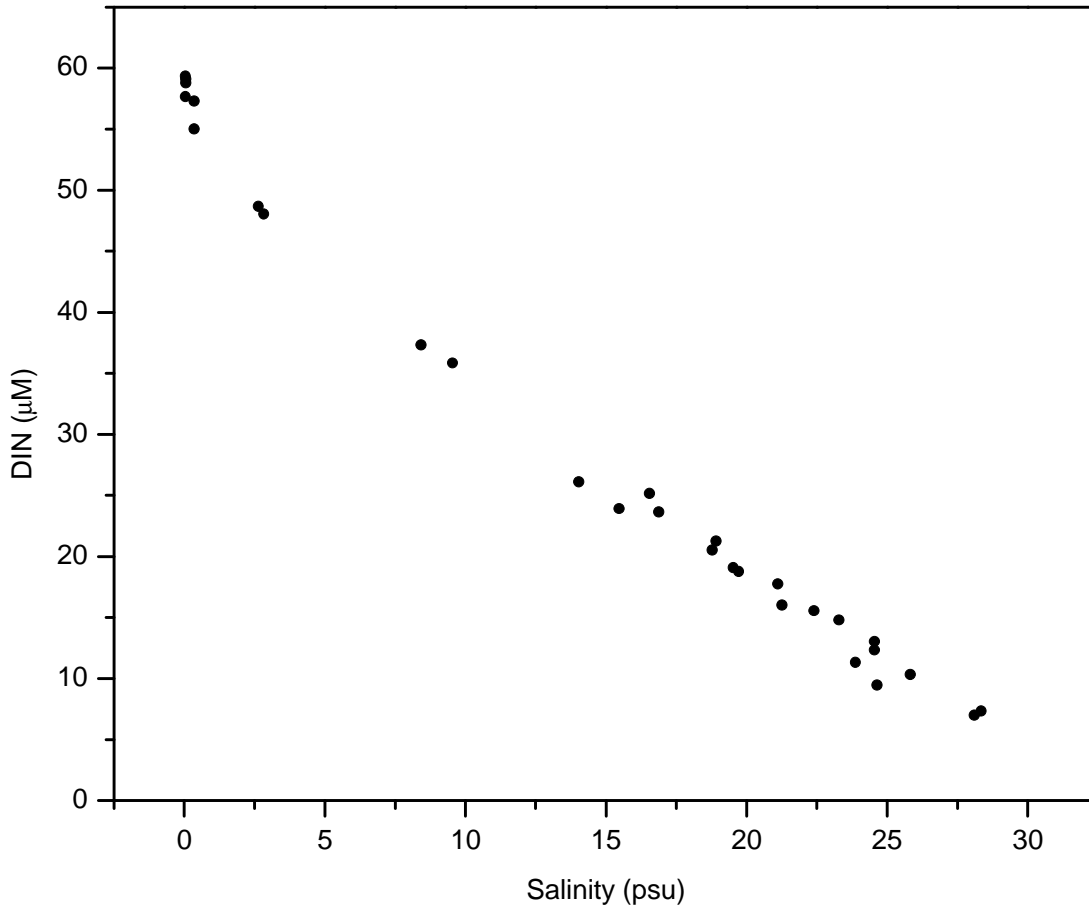


Figure 10. Example of a mixing diagram showing a riverine DIN source (generated using cruise data from May 6, 2003).

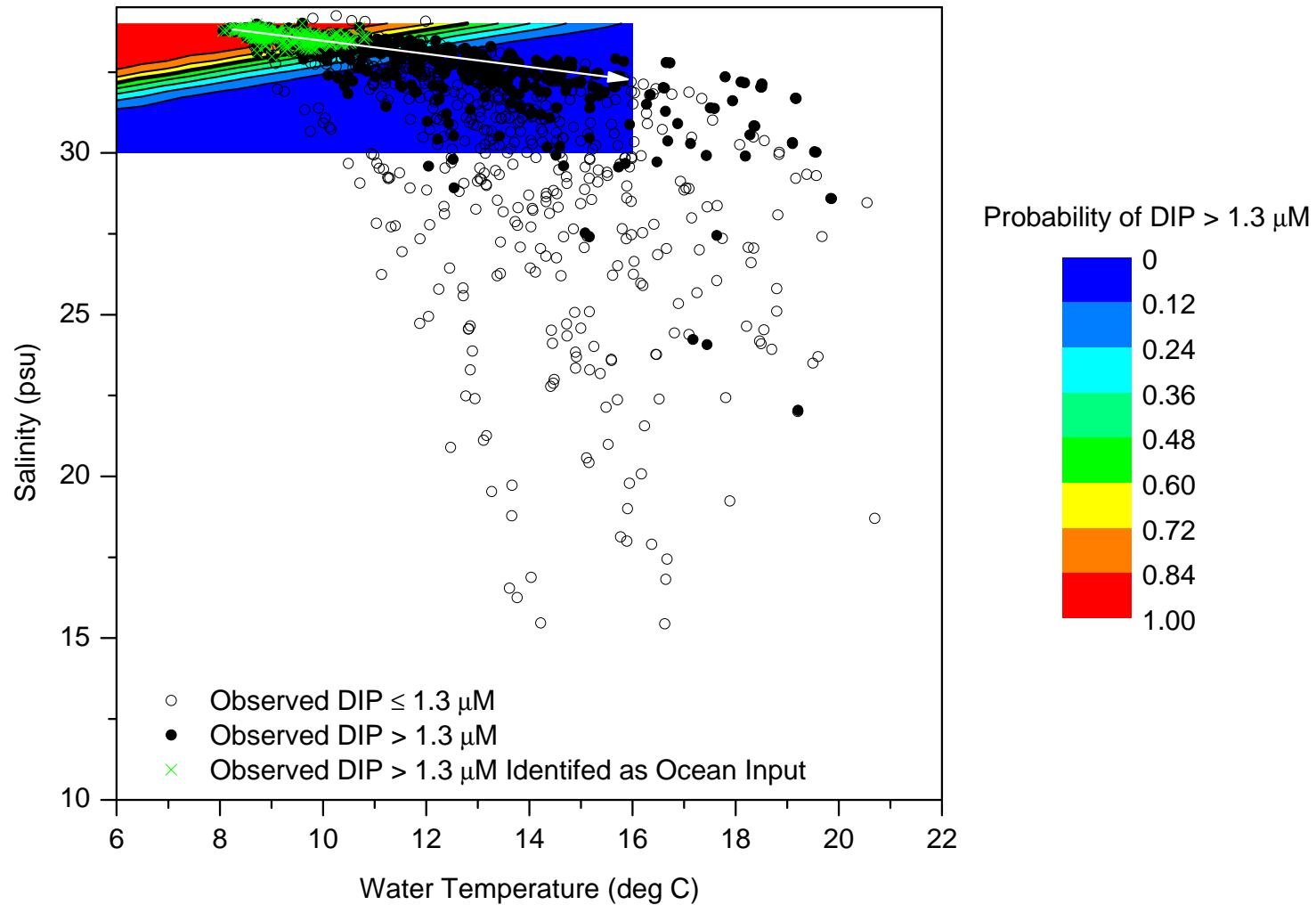


Figure 11. Temperature and salinity of cruise data measured in the Yaquina Estuary during the dry seasons of 1998-2008 with DIP  $\leq$  1.3  $\mu\text{M}$  (open circles) and DIP > 1.3  $\mu\text{M}$  (filled circles), and contours of probability of DIP > 1.3  $\mu\text{M}$  generated from logistic regression model with water temperature and salinity as explanatory variables. The green “x” symbols are observations of DIP > 1.3  $\mu\text{M}$  identified as ocean input from the logistic regression model with a prediction point of 0.60. The white arrow indicates a heating and mixing line.

because the ocean is the primary source of DIP.

One of the limitations of using logistic regression models to calculate the probability of an exceedance being due to ocean conditions is that the cool, high nutrient oceanic water warms up and mixes with low salinity and warm water both inside the estuary and on the shelf, reducing the distinctive thermohaline signature. Studies from the Oregon shelf off of Newport have demonstrated that most of the water that upwells is Subarctic water, which has salinity ranging from 32.5 to 33.8 psu and similar peak nutrients as those entering the estuary (Wheeler, et al. 2003; Huyer et al., 2005). In addition, the Columbia river plume influences shelf water off of Newport, with plume water having salinity < 32.5 psu. Offshore of Newport (80 km), the mean summer time water temperature is about 17°C and water temperatures off of Newport are strongly influenced by mixing, upwelling and advection (Huyer et al., 2005). Those samples identified as being associated with ocean input are a conservative estimate, and other observed exceedances that fall along the white arrows in Figures 9 and 11 are probably associated with upwelled ocean water that has heated and mixed with lower salinity water. Along this line, there is relatively large change in temperature (~ 8 °C) , and a relatively small change in salinity (2 psu), suggesting that heating dominates. A portion of this heating and mixing is occurring on the shelf and some is occurring inside the estuary.

#### *Alternate Approach – Using lagged flood tide data*

An alternate approach to identify exceedances associated with ocean input is to calculate the probability using water temperature and salinity from the previous flood tide. Values for temperature and salinity at the time of nutrient sampling are compared to those from the previous flood tide for May- October 2008 (Table 6), together with the probabilities calculated from the logistic regression using conditions at time of sampling and for the previous flood tide. As an example the sampling on May 15, 2008 shows an event where the nitrogen and phosphorous water quality thresholds were exceeded. However, the logistic regression model calculated using the water temperature and salinity at time of sampling would not classify this sampling event as an exceedance associated with ocean conditions. In contrast, the use of data from the previous flood-tide would identify the event as an exceedance associated with ocean input. Of the 8 observed exceedances of the DIN threshold during May – September 2008, the logistic regression model using temperature and salinity at time of sampling identified 4 as being

associated with ocean input, while by using the temperature and salinity from the previous flood tide, an additional 3 of the exceedances would be identified as being associated with ocean input (Table 6). Of the 9 exceedances of the DIP threshold, using temperature and salinity at time of sampling identified 5 as being associated with ocean input, while by using data from the previous flood tide, an additional 2 would be identified as being related to ocean input. However, using the previous flood-tide temperature and salinity combined with the logistic regression model would incorrectly indicate that 6 of the DIN and DIP observations less than threshold would be expected to exceed the threshold.

Table 6. Observed DIN and DIP, water temperature and salinity, and probability of exceeding nutrient thresholds calculated using water temperature and salinity at time of sampling and previous flood tide. The shaded observed nutrient cells identify those that exceeded the nutrient threshold, and the shaded probability cells are those that exceeded the optimal prediction point.

Sampling Date	Observed		Time of Sampling		Previous Flood Tide		Probability of Exceeding Nutrient Threshold Calculated Using Conditions from:			
	DIN ( $\mu\text{M}$ )	DIP ( $\mu\text{M}$ )	Temperature (deg C)	Salinity (psu)	Temperature (deg C)	Salinity (psu)	Time of Sampling		Previous Flood Tide	
							DIN	DIP	DIN	DIP
5/1/2008	1.6	0.22	9.8	30.7	9.8	30.9	0.01	0.00	0.02	0.00
5/9/2008	32.0	1.80	8.6	33.6	8.6	33.6	0.92	0.94	0.92	0.94
5/15/2008	22.2	1.56	12.4	31.2	9.0	33.5	0.00	0.00	0.85	0.87
5/21/2008	21.5	1.62	9.8	33.1	9.8	33.0	0.53	0.50	0.52	0.49
6/9/2008	14.5	0.81	13.4	26.3	10.1	33.3	0.00	0.00	0.58	0.61
6/26/2008	10.1	1.20	14.5	30.0	8.1	34.1	0.00	0.00	0.98	0.99
6/27/2008	10.3	1.29	14.7	30.5	8.5	34.2	0.00	0.00	0.97	0.99
6/30/2008	9.4	0.94	11.6	32.6	10.8	33.8	0.08	0.06	0.66	0.81
7/2/2008	10.5	1.12	13.7	31.9	12.1	33.6	0.00	0.00	0.27	0.41
7/16/2008	29.8	2.13	8.9	33.7	8.7	33.8	0.90	0.93	0.93	0.95
7/24/2008	25.6	1.88	9.2	33.4	8.7	34.5	0.79	0.81	0.98	0.99
7/31/2008	6.3	0.69	10.3	34.2	10.3	34.3	0.89	0.96	0.89	0.96
8/7/2008	13.9	1.47	10.7	33.9	9.8	34.2	0.72	0.85	0.91	0.97
8/12/2008	9.3	0.99	12.0	34.1	13.0	34.0	0.53	0.78	0.26	0.54
8/22/2008	10.8	1.42	13.9	32.4	14.0	32.5	0.01	0.01	0.01	0.01
8/26/2008	6.7	1.13	15.1	32.3	14.3	32.5	0.00	0.00	0.01	0.00
9/5/2008	16.5	1.96	12.0	31.0	9.4	33.5	0.00	0.00	0.78	0.82
9/10/2008	33.5	2.65	8.9	33.5	8.9	33.5	0.86	0.88	0.87	0.90
9/18/2008	5.6	0.74	10.6	34.1	10.4	34.2	0.82	0.92	0.85	0.94
9/23/2008	9.1	1.06	10.8	34.1	10.6	34.1	0.01	0.00	0.02	0.00

*Alternate Approach - Using Modeled Flood-Tide Nutrients*

Nelson and Brown (2008) present equations to model  $\text{NO}_3^- + \text{NO}_2^-$  and  $\text{PO}_4^{-3}$  levels using water temperature (generated using inner shelf data from Wetz et al. (2005)). Presented in Table 7 are observed and modeled median values for  $\text{NO}_3^- + \text{NO}_2^-$  and  $\text{PO}_4^{-3}$  calculated using water temperature at time of nutrient sampling and water temperature during the flood tide previous to the nutrient sampling for data collected at station Y1 during May to October 2008. The observed nutrients are significantly higher than those modeled using water temperature at time of sampling (Mann Whitney Rank Sum,  $p = 0.05$ ), but there is not a significant difference between observed values and those modeled using flood-tide water temperatures, suggesting that observed nutrients are a result of ocean input. This analysis suggests that comparing observed nutrients to those modeled using flood-tide water temperatures may be an alternate approach to determine if observed nutrient levels are consistent with ocean input.

34

Table 7. Observed median $\text{NO}_3^- + \text{NO}_2^-$ and $\text{PO}_4^{-3}$ for May – September 2008 and modeled using water temperature at time of sampling and water temperature during flood tide previous to sampling. Modeled values are calculated using the equations in Nelson and Brown (2008). N=20.			
Nutrient	Observed Median ( $\mu\text{M}$ )	Modeled Median ( $\mu\text{M}$ ) Calculated Using	
		Temperature at Time of Sampling	Flood Tide Temperature
$\text{NO}_3^- + \text{NO}_2^-$	7.9	3.7	9.1
$\text{PO}_4^{-3}$	1.3	0.9	1.3

### 3.2.2 Dissolved Oxygen

Dissolved oxygen levels in the lower portion of Yaquina Estuary are also influenced by upwelling conditions on the inner shelf. Figure 12 shows flood-tide dissolved oxygen levels at station Y1 as a function of a) temperature and salinity and b) density and *in situ* fluorescence. Low dissolved oxygen levels ( $< 5 \text{ mg l}^{-1}$ ) tend to occur at cool water temperatures (8-10 deg C), high salinities (32.5-34.5 psu), high water densities (sigma-t values  $> 25 \text{ kg m}^{-3}$ ), and are associated with low *in situ* fluorescence ( $< 5 \text{ } \mu\text{g l}^{-1}$ ), all of which are characteristics of recently upwelled water (Pearson and Holt, 1960; Park et al., 1962; Bourke and Pattulo, 1975; Brown and Power, in review). Occurrences of relatively high dissolved oxygen levels ( $> 6.5 \text{ mg l}^{-1}$ ) that occur at high water densities (sigma-t  $> 25 \text{ kg m}^{-3}$ ) also tend to have relatively high *in situ* fluorescence (an indicator of phytoplankton chlorophyll *a* levels). In this dataset, flood-tide dissolved oxygen was less than  $6.5 \text{ mg l}^{-1}$  (State of Oregon criterion for estuarine waters) 38% of the time at station Y1.

#### *Logistic Regression*

We used flood-tide dissolved oxygen data collected at station Y1 in the Yaquina Estuary (Figure 12) to generate logistic regression models, which predict the probability of dissolved oxygen levels  $< 6.5 \text{ mg l}^{-1}$ . Logistic regression models were generated for four sets of explanatory variables: 1) water temperature, 2) water temperature and salinity, 3) sigma-t, and 4) water temperature, salinity and *in situ* fluorescence. Due to diel fluctuations in dissolved oxygen levels, time of day is usually included in regression models of dissolved oxygen; however, our analysis did not indicate that time of day was a significant explanatory variable in these logistic models. The logistic regression models, standard errors and p-values are presented in Table 8.

The AUC values and optimal prediction points for the logistic regression models generated for the dissolved oxygen threshold are presented in Table 9. All of the models developed for dissolved oxygen had ‘excellent’ discrimination capability; however, there was improvement in model performance with the addition of *in situ* fluorescence. *In situ* fluorescence data were not available in 2002 and 2003; therefore, there is a large difference in sample size between the models that include fluorescence and those that exclude it (Table 9). The water temperature and water temperature and salinity models were re-calculated using the subset of data used for the model which includes *in situ*

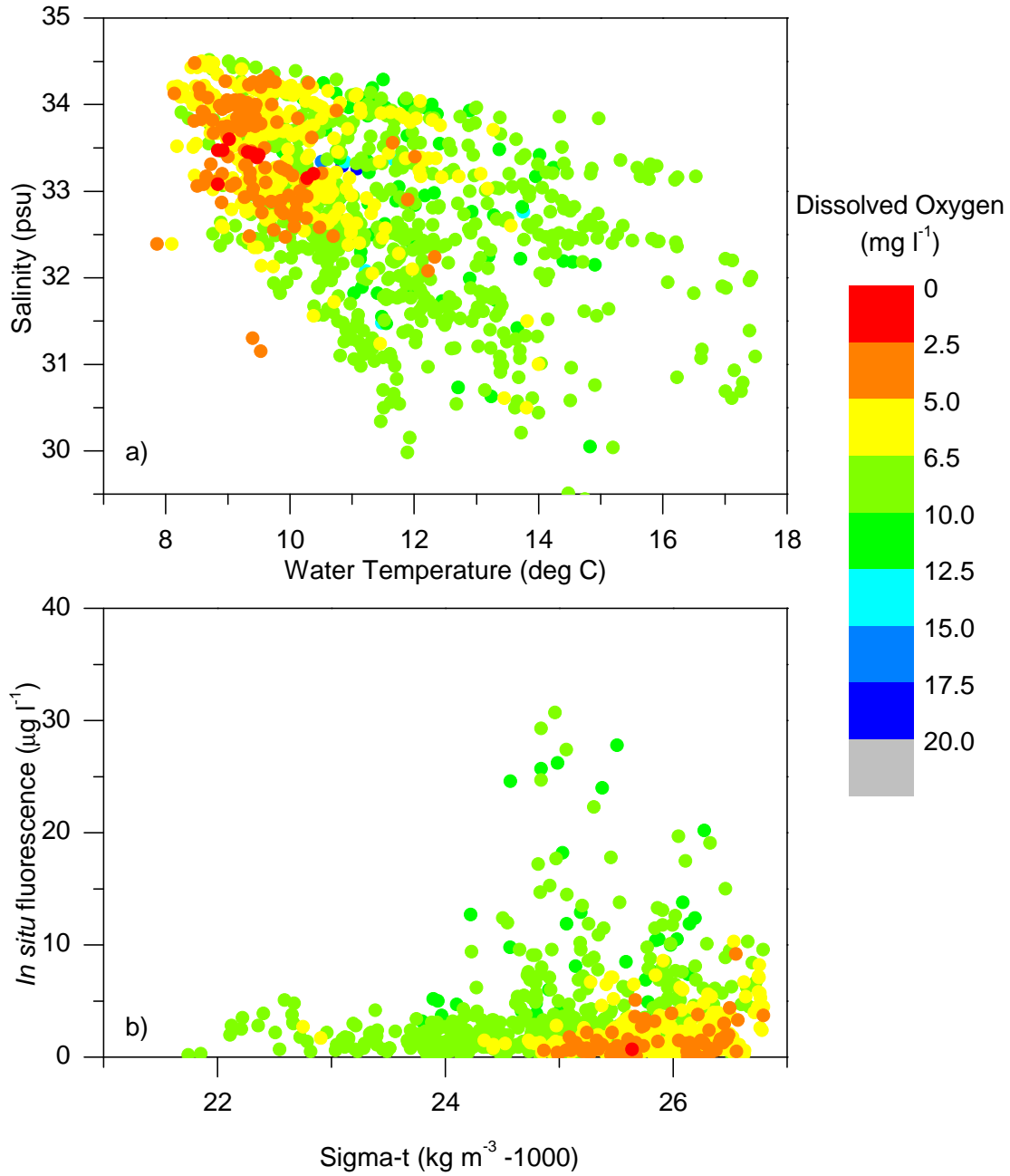


Figure 12. Flood-tide dissolved oxygen at station Y1 in the Yaquina Estuary plotted versus a) temperature and salinity, and b) sigma-t and *in situ* fluorescence. The upper panel included flood-tide data from May-October of 2002, 2003, 2004, 2007, and 2008. The lower panel includes data from May-October of 2004, 2007, and 2008.

fluorescence. These re-calculated values resulted in AUC values of 0.85 similar to those obtained for the full dataset indicating that sample size was not producing the difference in AUC values presented in Table 9. The false negative and false positive rates as a function of prediction point for the water temperature and salinity logistic regression model are presented in Figure 13 and the classification table is presented in Table A3.

Combining the optimal prediction points and the equation for the dissolved oxygen logistic regression, using only water temperature as the explanatory variable, results in a cutpoint of 10.3 °C for occurrences of dissolved oxygen < 6.5 mg l<sup>-1</sup> as predictive of ocean input. A sigma-t value of 25.4 kg m<sup>-3</sup> represents the density cutpoint for the occurrence of dissolved oxygen level < 6.5 mg l<sup>-1</sup> consistent with ocean input.

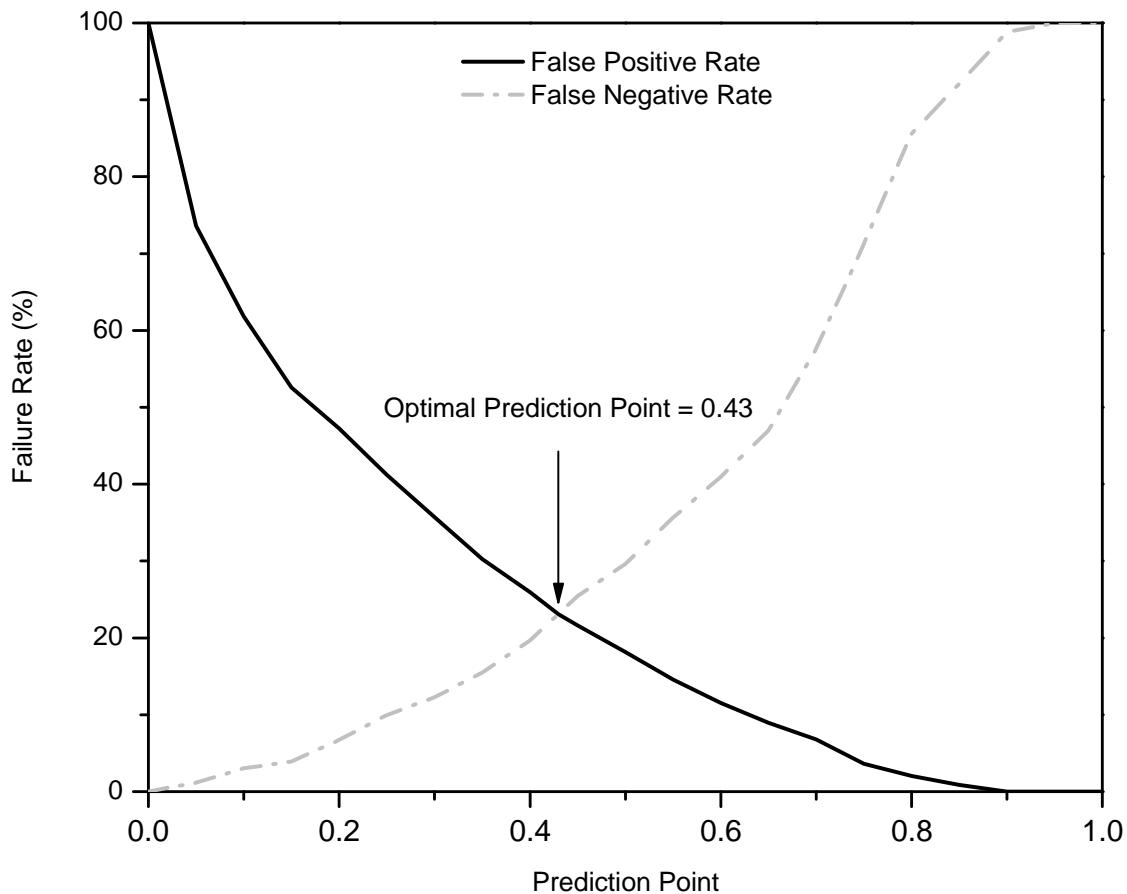


Figure 13. False positive and false negative rates as a function of prediction point for the logistic regression model for dissolved oxygen < 6.5 mg l<sup>-1</sup> using water temperature and salinity as explanatory variables. Optimal prediction point (0.43) is where overall failure rate is minimized and is located at the intersection of the two curves.

Table 8. Intercepts and coefficients for logistic regression models for occurrences of dissolved oxygen <math><6.5 \text{ mg l}^{-1}</math>.			
	Parameter	Standard error	p value
<b>Dissolved oxygen &lt;math&gt;&lt;6.5 \text{ mg l}^{-1}&lt;/math&gt; using water temperature</b>			
Intercept	10.47223	0.72229	$p < 0.001$
Water temperature	-1.03563	0.06999	$p < 0.001$
<b>Dissolved oxygen &lt;math&gt;&lt;6.5 \text{ mg l}^{-1}&lt;/math&gt; using water temperature and salinity</b>			
Intercept	-13.08966	3.95360	$p < 0.001$
Water temperature	-0.84449	0.07281	$p < 0.001$
Salinity	0.65113	0.10986	$p < 0.001$
<b>Dissolved oxygen &lt;math&gt;&lt;6.5 \text{ mg l}^{-1}&lt;/math&gt; using sigma-t</b>			
Intercept	-42.5248	2.8411	$p < 0.001$
Sigma-t	1.6589	0.1114	$p < 0.001$
<b>Dissolved oxygen &lt;math&gt;&lt;6.5 \text{ mg l}^{-1}&lt;/math&gt; using water temperature, salinity, and <i>in situ</i> fluorescence</b>			
Intercept	-23.59785	6.25981	$p < 0.001$
Water temperature	-0.84656	0.09254	$p < 0.001$
Salinity	1.00692	0.17905	$P < 0.001$
<i>In situ</i> fluorescence	-0.47812	0.05780	$p < 0.001$

Table 9. Sample size and area under the receiver operating characteristic curve (AUC) for the dissolved oxygen models. The optimal prediction points where false negative and false positive rates are equal are presented for each model.			
Model	N	AUC	Optimal Prediction Point
Dissolved oxygen <math><6.5 \text{ mg l}^{-1}</math> using water temperature	1126	0.84	0.44
Dissolved oxygen <math><6.5 \text{ mg l}^{-1}</math> using water temperature and salinity	1126	0.85	0.43
Dissolved oxygen <math><6.5 \text{ mg l}^{-1}</math> using sigma-t	1126	0.82	0.41
Dissolved oxygen <math><6.5 \text{ mg l}^{-1}</math> using water temperature, salinity, and <i>in situ</i> fluorescence	760	0.90	0.47

*Model Validation*

The predictive capability of each of the dissolved oxygen models was tested using flood-tide dissolved oxygen, temperature, salinity, and *in situ* fluorescence data collected at station Y1 from May-September 2009. For model validation, we used the water temperature and salinity model as well as the one that included *in situ* fluorescence. For this analysis, we used the optimal prediction point where the false positive and the false negative rates were equal. Tables 10 and 11 show the number of times the logistic regression model correctly and incorrectly predicted flood-tide dissolved oxygen falling below 6.5 mg l<sup>-1</sup> for the 2009 dataset. The logistic regression model including temperature and salinity had an overall accuracy of 79.8%, while the one including these variables and *in situ* fluorescence had an accuracy of 88.9%. Including *in situ* fluorescence in the logistic regression model resulted in a reduction of false positives by almost a factor of 2. The sensitivity and specificity of the logistic regression model including temperature and salinity were 90.3% and 75%, respectively. Inclusion of *in situ* fluorescence increased the sensitivity and specificity to 93.5% and 86.8%, respectively.

Table 10. Classification table showing accuracy of the water temperature and salinity logistic regression equation for predicting the occurrence of flood-tide dissolved oxygen < 6.5 mg l<sup>-1</sup> using data collected during May – September 2009 at station Y1. Prediction point = 0.43.

		Predicted Occurrence of Dissolved Oxygen		Total
		≥ 6.5 mg l <sup>-1</sup>	< 6.5 mg l <sup>-1</sup>	
Observed Occurrence of Dissolved Oxygen	≥ 6.5 mg l <sup>-1</sup>	51	17	68
	< 6.5 mg l <sup>-1</sup>	3	28	31
Total		54	45	99

Table 11. Classification table showing accuracy of the water temperature, salinity, and *in situ* fluorescence logistic regression equation for predicting the occurrence of flood-tide dissolved oxygen < 6.5 mg l<sup>-1</sup> using data collected during May – September 2009 at station Y1. Prediction point = 0.47.

		Predicted Occurrence of Dissolved Oxygen		Total
		≥ 6.5 mg l <sup>-1</sup>	< 6.5 mg l <sup>-1</sup>	
Observed Occurrence of Dissolved Oxygen	≥ 6.5 mg l <sup>-1</sup>	59	9	68
	< 6.5 mg l <sup>-1</sup>	2	29	31
Total		61	38	99

*Demonstration of Application of Logistic Regression Model*

We used additional datasets obtained from the Yaquina, Coos, Umpqua, Tillamook and Siletz estuaries to see how effective the logistic regression models were at identifying occurrences of dissolved oxygen less than 6.5 mg l<sup>-1</sup> associated with ocean input.

**Yaquina Estuary**

The water temperature and salinity logistic regression presented in Table 8 was applied to cruise data collected in the lower portion of Yaquina Estuary during the dry seasons of 2006 and 2007. If the probability calculated from the logistic regression exceeded the prediction point of 0.43, then the model predicted that dissolved oxygen would be less 6.5 mg l<sup>-1</sup> due to ocean conditions.

The logistic regression model identified 35 (or 73%) of the 48 occurrences of dissolved oxygen less than 6.5 mg l<sup>-1</sup> as being associated with ocean input (Figure 14). The median dissolved oxygen of the entire 2006 and 2007 cruise dataset was 6.9 mg l<sup>-1</sup> (n = 159). Removing the observations which the logistic model predicts would have a dissolved oxygen less than 6.5 mg l<sup>-1</sup> results in a median value of 7.4 mg l<sup>-1</sup> (n = 110). The logistic model should not identify all of the occurrences of dissolved oxygen less than the threshold because there may be other causes of low dissolved oxygen conditions. There are some events of dissolved oxygen < 6.5 mg l<sup>-1</sup> which the model does not

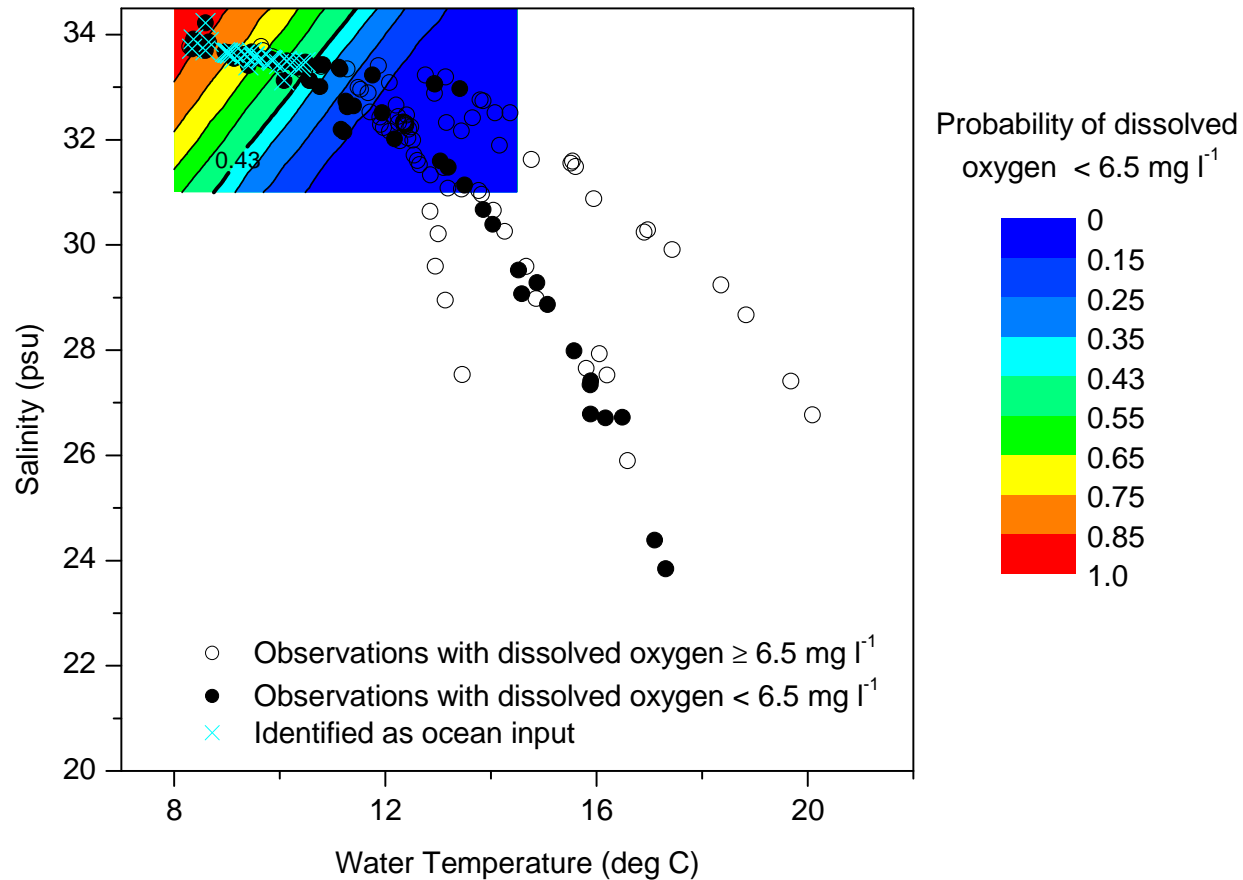


Figure 14. Temperature and salinity of cruise data measured in the Yaquina Estuary during May to October of 2006 and 2007 with dissolved oxygen  $\geq 6.5 \text{ mg l}^{-1}$  (open circles) and dissolved oxygen  $< 6.5 \text{ mg l}^{-1}$  (filled symbols), and contours of probability of dissolved oxygen  $< 6.5 \text{ mg l}^{-1}$  generated from the logistic regression model with water temperature and salinity as explanatory variables. The “x” symbols are those identified as ocean input from the logistic regression model with a prediction point of 0.43.

attribute to ocean input (filled symbols outside of the colored region); however, mixing diagrams (salinity versus dissolved oxygen plots) demonstrate that there was also an up estuary source of low dissolved oxygen during this period.

### **Coos Bay**

As an additional test of the logistic regression model at predicting events of dissolved oxygen  $<6.5 \text{ mg l}^{-1}$ , we applied the water temperature and salinity logistic regression to continuous data from the South Slough National Estuarine Research Reserve for a location near the entrance of Coos Bay during the period of June-September, 2006. Flood-tide temperature, salinity and dissolved oxygen values were identified and extracted from this dataset. The flood-tide data from Coos Bay exhibited similar patterns to the flood-tide data from Yaquina Estuary, with low dissolved oxygen levels occurring at cool water temperatures and high salinities (similar to Figure 12). Flood-tide dissolved oxygen levels were  $<6.5 \text{ mg l}^{-1}$  about 39% of the time. The logistic regression model (developed using water temperature and salinity generated using flood-tide data from the Yaquina Estuary) identified 45% of these events in Coos Bay as being associated with ocean input.

### **Classification Dataset**

The classification dataset was used to determine if the logistic regressions generated using data from the Yaquina Estuary would be applicable to other estuaries in the region. During a deployment near the entrance of the Siletz Estuary, 40% of the observations had dissolved oxygen values of  $< 6.5 \text{ mg l}^{-1}$ , and 93% of these observations were predicted to be associated with ocean input. During a deployment near the entrance of the Umpqua Estuary, 29% of the observations had dissolved oxygen values of  $< 6.5 \text{ mg l}^{-1}$ , and 60% of these observations were predicted by the logistic regression model to be related to ocean input. During a deployment near the mouth of Tillamook Estuary, 43% of the observations had dissolved oxygen values  $< 6.5 \text{ mg l}^{-1}$ , and 49% of these observations were predicted to be associated with ocean input. Based on these results, we believe that the logistic models developed in this report may be applicable to other estuaries in the region.

#### 4. Summary

Observations from the Yaquina and other estuaries in the Pacific Northwest show that intrusions of coastal ocean water into the estuaries can result in high nitrogen ( $\sim 32 \mu\text{M}$ ), phosphorous ( $\sim 3 \mu\text{M}$ ), and chlorophyll *a* levels (up to  $50 \mu\text{g l}^{-1}$ ), and low dissolved oxygen (at times  $< 2 \text{ mg l}^{-1}$ ) conditions. These natural intrusions of oceanic water into PNW estuaries thus often have values of water quality parameters that exceed water quality criteria, or are greater than values for eutrophication indicators associated with highly eutrophic status (e.g., Bricker et al., 2003). Many states, including Washington and Oregon, have a narrative criterion that specifies that if natural conditions are the cause of non-attainment of a water quality standard, then the natural conditions become the standard; thus, tools that identify natural events that will cause non-attainment of water quality standards are needed.

This report demonstrates an approach for distinguishing exceedances of water quality thresholds associated with ocean conditions by using logistic regression models. These types of models have been variously used to forecast the occurrence of poor water quality conditions within streams, estuaries, and the coastal ocean. For example, logistic regression models have been used to predict occurrences of toxic phytoplankton blooms in the coastal ocean (Lane et al., 2009), forecast non-attainments of water quality standards in an estuarine impoundment (Worrall et al., 1998), to predict the eutrophication status of estuaries (Lowery, 1998), to forecast the probability of exceedance of a turbidity criterion in streams (Towler et al., 2010), and to assess attainment of dissolved oxygen criteria in Chesapeake Bay (US EPA, 2003).

The logistic regression models presented in this report are simple tools, which provide the probability of an observation exceeding a water quality threshold due to ocean conditions based on water temperature, salinity, and *in situ* fluorescence (for dissolved oxygen) at time of sampling. It is possible to distinguish oceanic inputs due to their distinctive thermal and saline signatures. Typically, dissolved oxygen levels decrease with increasing temperature due to both reduced solubility of oxygen in water and due to increased respiration and decomposition (e.g., Lee and Lwiza, 2008; Verity et al., 2006). However, in the marine-dominated portion of Pacific Northwest estuaries, minimum dissolved oxygen values often occur at cool water temperatures, which are

distinctive from the water temperatures associated with within estuary causes of low dissolved oxygen. In addition, water masses with high nutrients associated with ocean input have temperatures and salinities which differ from those associated with riverine and point source inputs. Based on the analysis presented in this report, we suggest that water temperature and salinity data always be collected at the same time as nutrient and dissolved oxygen concentrations are measured.

To apply these regression models, the user would need to substitute the parameters in Tables 2 and 8 into Equation 1. The probability of exceedance being associated with ocean input is then calculated using Equation 2, and the value of Equation 1 calculated using the measured temperature, salinity and in situ fluorescence (for dissolved oxygen if available). The user then will need to provide the prediction point either using the optimal prediction point presented in Tables 3 and 9 or specifying a different prediction point based on the needs of their application. If the calculated probability is greater than the prediction point, then the exceedance is predicted to be associated with ocean input. The regression models presented in this report were calculated using the water quality thresholds presented in Table 1. If the user desired other water quality thresholds, then the logistic regression equations would need to be recalculated.

Occasionally, water masses with high chlorophyll *a* are advected into PNW estuaries from the coastal ocean (Brown and Ozretich, 2009). However, these phytoplankton blooms do not have as distinctive of a temperature and salinity signature as high nutrients or low dissolved oxygen events. This decrease in the distinctive signature occurs because peak chlorophyll *a* levels entering estuaries lag upwelling conditions by about 4 to 7 days (Brown and Ozretich, 2009). Phytoplankton blooms develop while upwelled water with high nutrient concentrations is exposed to sunlight and warms up. Therefore, we do not feel that this approach will be capable of distinguishing exceedances of chlorophyll *a* thresholds related to ocean input. However, Newton and Horner (2003) demonstrated that phytoplankton species can be used to identify the origin of phytoplankton blooms inside PNW estuaries, including those advected from the ocean.

Nutrient and dissolved oxygen observations identified as being due to ocean input should not be used in assessing compliance of water quality standards or for assessing eutrophication status (e.g., using the approach of Bricker et al. 2003). By excluding observations associated with ocean input from water body assessments, type I errors in listings (i.e., falsely listing a segment as impaired when it isn't) may be reduced. Falsely declaring an estuarine reach as impaired results in unnecessary planning and costs (Smith et al., 2001). Logistic regression models such as those presented in this report could also be used to remove the effect of ocean input in a water quality dataset, and then the remaining data could be used in the development of nutrient criteria (e.g., using the percentile approach presented in Brown et al. (2007).

For estuarine assessments, such as the EPA's National Coastal Assessment (EPA, 2004), water quality is assessed as "good", "fair" or "poor" by comparing observed water quality indicators to thresholds established for each of these categories. For example, for the west coast of the United States, the thresholds for DIP in the last National Coastal Assessment were as follows:  $DIP < 0.32 \mu\text{M}$  were rated as "good",  $0.32 \mu\text{M} \leq DIP \leq 3.2 \mu\text{M}$  were rated as "fair", and  $DIP > 3.2 \mu\text{M}$  were rated as "poor." In the most recent assessment of west coast estuaries, 86% of the sites had DIP levels in the "fair" category, and 10% in the "poor" category (EPA, 2004). This report also states that coastal upwelling may have been an important contributing factor to the high DIP levels. In the flood-tide dataset from the Yaquina Estuary, 91% of the DIP observations would be classified as "fair", and 9% as "good" using the National Coastal Assessment threshold. In this report, we present logistic regression models for the thresholds presented in Table 1; however, additional logistic regressions could be developed for other water quality thresholds such as those used in EPA (2004) and Bricker et al. (2003). An alternate approach would be to use flood-tide or inner shelf data to develop thresholds for the categories that are a function of water temperature and salinity. Based on the data presented in this report, the nutrient thresholds for the water quality indicators would need to be increased and the dissolved oxygen threshold decreased at low water temperatures and high salinities due to the influence of coastal upwelling.

The logistic regression models developed in this report may be applicable at a regional scale for estuaries extending from northern California to outer coast estuaries

along the Washington coast. If the models presented in this report were applied to other Oregon estuaries, this would require the assumption that the nutrient and dissolved oxygen levels and their distinctive thermal and saline signatures are uniform along the coast. More extensive verification of the approach would be needed prior to applying these models to other estuaries. In addition, this method also assumes that the nutrient and oxygen levels entering the Yaquina Estuary are related to coastal upwelling, rather than being influenced by plume effects or runoff from coastal watersheds. The Columbia River plume has been shown to influence the coastal ocean along the Oregon shelf; however, Huyer et al (2005) found that there is no evidence that the plume supplies any nitrates to the region off of Newport. In addition, peak flood tide nutrient concentrations entering the Yaquina during dry season flood tides are consistent with recently upwelled water on the shelf and strongly correlated with upwelling favorable wind stress (Brown and Ozretich, 2009). Based on these lines of evidence, we feel that nutrient and dissolved oxygen level in flood tide water entering the Yaquina Estuary results from upwelling processes rather than plume effects. For other estuaries that are in closer proximity Columbia River (such as Willapa Bay, WA), this may not be the case. These models would be most useful for tide-dominated estuaries in the Pacific Northwest, such as Coos, Yaquina and Tillamook Bays (Lee and Brown, 2009). This method may also be useful for distinguishing upwelling caused hypoxic events in other regions. For example, Glenn et al. (2004) suggested that recurrent hypoxia on the inner shelf off the coast of New Jersey is related to coastal upwelling.

The models developed in this report will not capture all of the oceanic import events, because as the water heats up and mixes with low salinity and warm water in the estuary, the ocean signature becomes obscured. Hence, exceedances identified as ocean input by the logistic regression models will be under-estimated. More work is required to incorporate the heating of cool ocean water both inside and outside the estuary. An alternate approach to deal with this limitation may be to use water temperature and salinity observations for the flood tide prior to observed sampling, or by comparing observed nutrients to modeled nutrient values using flood-tide water temperatures. Additionally, since both high nutrients and low dissolved oxygen conditions are characteristic of recently upwelled water, if there are exceedances of nitrogen,

phosphorous, and dissolved oxygen thresholds simultaneously during a sampling event, this may provide additional confidence in attributing these exceedances to ocean input.

The best predictor of dissolved oxygen events  $<6.5 \text{ mg l}^{-1}$  included *in situ* fluorescence. The models which excluded *in situ* fluorescence had more observations classified as false positives (i.e., modeled predicted dissolved oxygen  $< 6.5 \text{ mg l}^{-1}$ , while observed values exceeded this threshold). Worrall et al. (1998) found similar misclassification due to the presence of algal blooms when using a logistic regression model to predict exceedances of a dissolved oxygen criterion in an estuarine impoundment. We included this parameter in the model to demonstrate that *in situ* fluorescence (a measure of phytoplankton chlorophyll *a*) improves model performance. However, we caution against applying this specific logistic model to other datasets due to instrumentation and calibration differences in the measurement of *in situ* fluorescence. The specific equation would only be applicable to datasets that use the same YSI chlorophyll *a* sensor and calibration methods described in this report.

The traditional method of identifying nutrient sources or causes of low dissolved oxygen within estuaries is the use of mixing diagrams, which requires that end members (ocean and river) remain relatively constant (Loder and Reichard, 1981). Previous research has demonstrated high temporal variability in ocean conditions (Brown and Ozretich, 2009), with water quality conditions in the nearshore coastal ocean changing on the scales of hours to days, which prohibits creating mixing diagrams using data collected over multiple days. The use of mixing diagrams requires sampling multiple stations along the axis of the estuary within a short period of time. However, due to logistical constraints, water quality sampling is often random with respect to tidal stage, and often only a few locations are sampled within an estuary on a particular sampling date. One advantage of the approach presented in this report is that it can be used even when only one location in the estuary is sampled on a given day.

Many of the watersheds of PNW estuaries presently have relative low levels of development and human population density in their watersheds (Lee and Brown, 2009); however, populations are expected to increase. Similar to other regions of the United States (e.g., Crossett et al., 2004), highest human populations are located along the coast and adjacent to many PNW estuaries (Lee and Brown, 2009); hence it is desirable to

develop an approach that identifies water quality conditions associated with the coastal ocean. One can then remove those observations related to ocean conditions, and use the remaining data to assess the status of estuarine water quality conditions and to assess attainment of water quality standards. In addition, filtering out oceanic conditions from estuarine water quality datasets may aid in identifying other sources of water quality degradation. For example, often land uses in watersheds are correlated with water quality conditions within estuaries (e.g., Dauer et al., 2000; Kauppila et al., 2003). Development and highest population densities are often co-located adjacent to the most seaward portion of estuaries, adjacent to the portion of the estuarine system where ocean conditions are most likely to cause high nutrient, low dissolved oxygen, and high chlorophyll *a* conditions. If the influence of the coastal ocean is not removed from samples taken for compliance monitoring of water quality criteria, it may obscure anthropogenic effects and cause misinterpretation of results.

In order to make the application of the approach developed in this report as accessible as possible, we are presently developing a data exploration tool, which graphically displays user-provided data, and compares it to flood-tide data from Yaquina and the inner shelf, and identifies data points associated with ocean input using the logistic regression models presented in this report.

Some studies have suggested that future climate change may lead to changes in seasonality or intensity of coastal wind-driven upwelling (Snyder et al., 2003). It has recently been suggested that there has been an increase in the occurrence of severe hypoxic condition on the Oregon shelf (Chan et al., 2008). If future studies demonstrate anthropogenic-related changes in the amount of coastal upwelling or in the occurrence of hypoxia on the inner shelf, then those exceedances identified as associated with ocean input may have some component related to anthropogenic activities, which will greatly complicate decisions with regard to compliance monitoring for water quality criteria. New approaches will doubtlessly be required.

## 5. Literature Cited

- Barth, J.A., B.A. Menge, J. Lubchenco, F. Chan, J.M. Bane, A.R. Kirincich, M.A. McManus, K.J. Nielsen, S.D. Pierce, and L. Washburn. 2007. Delayed upwelling alters nearshore coastal ocean ecosystems in the northern California current. *Proceedings of the National Academy of Sciences*, 104(10):3719-3724, [www.pnas.org/cgi/doi/10.1073/pnas.0700462104](http://www.pnas.org/cgi/doi/10.1073/pnas.0700462104).
- Bourke, R.H. and J.G. Pattullo. 1974. Seasonal variation of the water mass along the Oregon-Northern California coast. *Limnology and Oceanography*, 19(2):190-198.
- Bricker, S.B., J.G. Ferreira, and T. Simas. 2003. An integrated methodology for assessment of estuarine trophic status. *Ecological Modelling*, 169:39-60.
- Brown, C.A., W.G. Nelson, B.L. Boese, T.H. DeWitt, P.M. Eldridge, J.E. Kaldy, H. Lee II, J.H. Power, and D.R. Young. 2007. An approach to developing nutrient criteria for Pacific Northwest estuaries: A case study of Yaquina Estuary, Oregon. US EPA, Washington, D.C., EPA/600/R-07/046. 183 pp.
- Brown, C.A. and R.J. Ozretich. 2009. Coupling between the coastal ocean and Yaquina Bay, Oregon: Importance of oceanic inputs relative to other nitrogen sources. *Estuaries and Coasts*, 32: 219-237, doi 10.1007/s12237-008-9128-6.
- Brown, C.A. and J.H. Power. In review. Historic and recent patterns in dissolved oxygen within the Yaquina Estuary (Oregon, USA): Importance of anthropogenic activities and oceanic conditions. Submitted to *Estuarine, Coastal and Shelf Science*.
- Chan, F., J.A. Barth, J. Lubchenco, A. Kirincich, A. Weeks, W.T. Peterson, and B.A. Menge. 2008. Emergence of anoxia in the California Current large marine ecosystem. *Science*, 319:920.
- Corwith, H.L. and P.A. Wheeler. 2002. El Niño related variations in nutrient and chlorophyll distributions off Oregon. *Progress in Oceanography*, 54:361-380.
- Crossett, K.M., T.J. Culliton, P.C. Wiley, and T.R. Goodspeed. 2004. Population trends along the coastal United States: 1980-2008. Coastal Trends Report Series. National Oceanic and Atmospheric Administration.
- Dauer, D.M., J.A. Ranasinghe, and S.B. Weisberg. 2000. Relationships between benthic community condition, water quality, sediment quality, nutrient loads, and land use patterns in Chesapeake Bay. *Estuaries*, 23(1): 80-96.
- De Angelis, M.A. and L.I. Gordon. 1985. Upwelling and river runoff as sources of dissolved nitrous oxide to the Alsea estuary, Oregon. *Estuarine, Coastal and Shelf Science*, 20:375-386.
- Donohue, R. and E. van Looij. 2001. The derivation of percentile quality criteria for the Swan-Canning Estuary; A binomial approach. Swan River Trust, Swan-Canning Cleanup Program Report SCCP 24.
- EPA. 2004. National Coastal Condition Report II. U.S. Environmental Protection Agency, Washington, DC., EPA-620/R-03/002. [www.epa.gov/owow/oceans/nccr2/](http://www.epa.gov/owow/oceans/nccr2/)
- Glenn, S., R. Arnone, T. Bergmann, W.P. Bissett, M. Crowley, J. Cullen, J. Gryzmski, D. Haidvogel, J. Kohut, M. Moline, M. Oliver, C. Orrico, R. Sherrell, T. Song, A. Weidemann, R. Chant, and O. Schofield. 2004. Biogeochemical impact of summertime coastal upwelling on the New Jersey Shelf. *Journal of Geophysical Research*, 109, C12S02, doi:10.1029/2003JC002265.

- Grantham, B.A., F. Chan, K.J. Nielsen, D.S. Fox, J.A. Barth, A. Huyer, J. Lubchenco, and B.A. Menge. 2004. Upwelling-driven nearshore hypoxia signals ecosystem and oceanographic changes in the northeast Pacific. *Nature*, 429:749-754.
- Haertel, L, C. Osterberg, H. Curl, Jr., and P.K. Park. 1969. Nutrient and plankton ecology of the Columbia River estuary. *Ecology*, 50(6):962-978.
- Hosmer, D.W. and S. Lemeshow. 2000. Applied logistic regression. 2<sup>nd</sup> edition, John Wiley, New York, NY.
- Huyer, A., J.H. Fleischbein, J. Keister, P. M. Kosro, N. Perlin, R.L. Smith, and P.A. Wheeler. 2005. Two coastal upwelling domains in the northern California Current system. *Journal of Marine Research*, 63:901-929.
- Kauppila, P., J.J. Meeuwig, and H. Pitkänen. 2003. Predicting oxygen in small estuaries of the Baltic Sea: a comparative approach. *Estuarine, Coastal and Shelf Science*, 57:1115-1126.
- Kosro, P.M. 2003. Enhanced southward flow over the Oregon shelf in 2002: A conduit for subarctic water. *Geophysical Research Letters*, 30(15): 8023, doi: 10.1029/2003GL017436.
- Lane, J.Q., P.T. Raimondi, and R.M. Kudela. 2009. Development of a logistic regression model for the prediction of toxigenic *Pseudo-nitzschia* blooms in Monterey Bay, California. *Marine Ecology Progress Series*, 383:37-51.
- Lee and C.A. Brown. 2009. Classification of Regional Patterns of Environmental Drivers and Benthic Habitats in Pacific Northwest Estuaries. USEPA, Washington, D.C., EPA/600/R-09/140. 298 pp.
- Lee, Y.J. and K.M.M. Lwiza. 2008. Characteristics of bottom dissolved oxygen in Long Island Sound, New York. *Estuarine, Coastal and Shelf Science*, 76(2):187-200.
- Loder, T.C. and R.P. Reichard. 1981. The dynamics of conservative mixing in estuaries. *Estuaries*, 4(1):64-69.
- Lowery, T.A. 1998. Modelling estuarine eutrophication in the context of hypoxia, nitrogen loadings, stratification and nutrient ratios. *Journal of Environmental Management*, 52, 289-305.
- Menge, B.A., F. Chan, K.J. Nielsen, E. Di Lorenzo, and J. Lubchenco. 2009. Climatic variation alters supply-side ecology: impact of climate patterns on phytoplankton and mussel recruitment. *Ecological Monographs*, 79(3):379-395.
- Nelson, W.G. and C.A. Brown. 2008. Use of probability-based sampling of water-quality indicators in supporting development of quality criteria. *ICES Journal of Marine Science*, 65:1421-1427.
- Newton, J.A. and R.A. Horner. 2003. Use of phytoplankton species indicators to track the origin of phytoplankton blooms in Willapa Bay, Washington. *Estuaries*, 26(4B): 1071-1078.
- Park, K., J.G. Pattullo, and B. Wyatt. 1962. Chemical properties as indicators of upwelling along the Oregon coast. *Limnology and Oceanography*, 7: 435-437.
- Pearson, E.A. and G.A. Holt. 1960. Water quality and upwelling at Grays Harbor entrance. *Limnology and Oceanography*, 5(1):48-56.
- Peterson, W.T., J.E. Keister, and L.R. Feinberg. 2002. The effects of the 1997-1999 El Niño/La Niña on hydrography and zooplankton off the central Oregon coast. *Progress in Oceanography*, 54:381-398.

- R Development Core Team (2008). R: A language and environment for statistical computing. R Foundation for Statistical Computing, Vienna, Austria. ISBN 3-900051-07-0, <http://www.R-project.org>.
- Roegner, G.C., B.M. Hickey, J.A. Newton, A.L. Shanks, and D.A. Armstrong. 2002. Wind-induced plume and bloom intrusions into Willapa Bay, Washington. *Limnology and Oceanography*, 47(4):1033-1042.
- Roegner, G. and A. Shanks. 2001. Import of coastally-derived chlorophyll *a* to South Slough, Oregon. *Estuaries*, 24:224-256.
- Smith, E.P., K. Ye, C. Hughes, and L. Shabman. 2001. Statistical assessment of violations of water quality standards under Section 303(d) of the Clean Water Act. *Environmental Science and Technology*, 35(3):606-612.
- Snyder, M.A., L.C. Sloan, N.S. Diffenbaugh, and J.L. Bell. 2003. Future climate change and upwelling in the California Current. *Geophysical Research Letters*, 30(15):1823. doi:10.1029/2003GL017647.
- Thomas, A.C., P.T. Strub, and P. Brickley. 2003. Anomalous satellite-measured chlorophyll concentrations in the northern California Current in 2001-2002. *Geophysical Research Letters*, 30(15):8022, doi:10.1029/2003GL017409,2003.
- Towler, E, B. Rajagopalan, R. S. Summers, and D. Yates. 2010. An approach for probabilistic forecasting of seasonal turbidity threshold exceedance. *Water Resources Research*, 46, W06511, doi:10.1029/2009WR007834, 2010.
- Verity, P.G., M. Alber, and S.B. Bricker. 2006. Development of hypoxia in well-mixed subtropical estuaries in the Southeastern USA. *Estuaries and Coasts* 29(4): 665-673.
- Wetz, J.J., J. Hill, H. Corwith, and P.A. Wheeler. 2005. Nutrient and extracted chlorophyll data from the GLOBEC long-term observation program, 1997-2004. Data Report 193, COAS Reference 2004-1, Oregon State University, Corvallis, Oregon.
- Wheeler, P.A., A. Huyer, and J. Fleischbein. 2003. Cold halocline, increased nutrients and higher chlorophyll off Oregon in 2002. *Geophysical Research Letters*, 30(15): 8021, doi:10.1029/2003GL017395,2003.
- Worrall, F., D.A. Wooff, and P. McIntyre. 1998. A simple modelling approach for water quality: The example of an estuarine impoundment. *The Science of the Total Environment*, 219:41-51.
- U.S. EPA. 2003. Ambient Water Quality Criteria for Dissolved Oxygen, Water Clarity and Chlorophyll *a* for the Chesapeake Bay and Its Tidal Tributaries. Appendix I: Analytical approaches for assessing short-duration dissolved oxygen criteria. USEPA, Washington, D.C., EPA 903-R-03-002.

## **Appendices**

Provided in the appendices are classification tables of the logistic regression models generated for DIN, DIP, and dissolved oxygen using water temperature and salinity.

Table A1. Classification table for DIN logistic regression with water temperature and salinity as explanatory variables for probability prediction points ranging from 0 to 1. The row that is shaded shows the optimal prediction point where false negative and false positive rates are approximately equal.

Prediction Point	Total Correct		Total Incorrect		Percent				
	DIN > 14 $\mu$ M	DIN $\leq$ 14 $\mu$ M	DIN > 14 $\mu$ M	DIN $\leq$ 14 $\mu$ M	Correct	Sensitivity	Specificity	False Positive	False Negative
0	194	0	0	237	45.0	100.0	0.0	100.0	0.0
0.05	193	147	1	90	78.9	99.5	62.0	38.0	0.5
0.10	193	159	1	78	81.7	99.5	67.1	32.9	0.5
0.15	190	167	4	70	82.8	97.9	70.5	29.5	2.1
0.20	189	173	5	64	84.0	97.4	73.0	27.0	2.6
0.25	188	180	6	57	85.4	96.9	75.9	24.1	3.1
0.30	185	186	9	51	86.1	95.4	78.5	21.5	4.6
0.35	181	188	13	49	85.6	93.3	79.3	20.7	6.7
0.40	176	191	18	46	85.2	90.7	80.6	19.4	9.3
0.45	173	193	21	44	84.9	89.2	81.4	18.6	10.8
0.50	169	198	25	39	85.2	87.1	83.5	16.5	12.9
0.55	163	200	31	37	84.2	84.0	84.4	15.6	16.0
0.60	161	204	33	33	84.7	83.0	86.1	13.9	17.0
0.65	156	209	38	28	84.7	80.4	88.2	11.8	19.6
0.70	148	214	46	23	84.0	76.3	90.3	9.7	23.7
0.75	143	221	51	16	84.5	73.7	93.2	6.8	26.3
0.80	133	224	61	13	82.8	68.6	94.5	5.5	31.4
0.85	112	228	82	9	78.9	57.7	96.2	3.8	42.3
0.90	78	237	116	0	73.1	40.2	100.0	0.0	59.8
0.95	40	237	154	0	64.3	20.6	100.0	0.0	79.4
1.00	0	237	194	0	55.0	0.0	100.0	0.0	100.0

Table A2. Classification table for DIP logistic regression with water temperature and salinity as explanatory variables for probability prediction points ranging from 0 to 1. The row that is shaded shows the optimal prediction point where false negative and false positive rates are approximately equal.

Prediction Point	Total Correct		Total Incorrect		Percent				
	DIP > 1.3 $\mu$ M	DIP $\leq$ 1.3 $\mu$ M	DIP > 1.3 $\mu$ M	DIP $\leq$ 1.3 $\mu$ M	Correct	Sensitivity	Specificity	False Positive	False Negative
0	204	0	0	227	47.3	100.0	0.0	100.0	0.0
0.05	203	154	1	73	82.8	99.5	67.8	32.2	0.5
0.10	202	166	2	61	85.4	99.0	73.1	26.9	1.0
0.15	200	170	4	57	85.8	98.0	74.9	25.1	2.0
0.20	199	175	5	52	86.8	97.5	77.1	22.9	2.5
0.25	198	180	6	47	87.7	97.1	79.3	20.7	2.9
0.30	197	187	7	40	89.1	96.6	82.4	17.6	3.4
0.35	195	188	9	39	88.9	95.6	82.8	17.2	4.4
0.40	193	191	11	36	89.1	94.6	84.1	15.9	5.4
0.45	191	194	13	33	89.3	93.6	85.5	14.5	6.4
0.50	188	195	16	32	88.9	92.2	85.9	14.1	7.8
0.55	185	197	19	30	88.6	90.7	86.8	13.2	9.3
0.60	181	200	23	27	88.4	88.7	88.1	11.9	11.3
0.65	176	203	28	24	87.9	86.3	89.4	10.6	13.7
0.70	169	205	35	22	86.8	82.8	90.3	9.7	17.2
0.75	158	207	46	20	84.7	77.5	91.2	8.8	22.5
0.80	149	212	55	15	83.8	73.0	93.4	6.6	27.0
0.85	142	215	62	12	82.8	69.6	94.7	5.3	30.4
0.90	118	225	86	2	79.6	57.8	99.1	0.9	42.2
0.95	62	227	142	0	67.1	30.4	100.0	0.0	69.6
1.00	0	227	204	0	52.7	0.0	100.0	0.0	100.0

Table A3. Classification table for dissolved oxygen logistic regression with water temperature and salinity as explanatory variables for probability prediction points ranging from 0 to 1. The row that is shaded shows the optimal prediction point where false negative and false positive rates are approximately equal.

Prediction Points	Total Correct		Total Incorrect		Percent				
	< 6.5 mg l <sup>-1</sup>	≥ 6.5 mg l <sup>-1</sup>	< 6.5 mg l <sup>-1</sup>	≥ 6.5 mg l <sup>-1</sup>	Correct	Sensitivity	Specificity	False Positive	False Negative
0	432	0	0	694	38.4	100.0	0.0	100.0	0.0
0.05	427	183	5	511	54.2	98.8	26.4	73.6	1.2
0.1	419	265	13	429	60.7	97.0	38.2	61.8	3.0
0.15	415	329	17	365	66.1	96.1	47.4	52.6	3.9
0.2	403	366	29	328	68.3	93.3	52.7	47.3	6.7
0.25	389	408	43	286	70.8	90.0	58.8	41.2	10.0
0.3	379	446	53	248	73.3	87.7	64.3	35.7	12.3
0.35	365	484	67	210	75.4	84.5	69.7	30.3	15.5
0.4	347	514	85	180	76.5	80.3	74.1	25.9	19.7
0.43	332	534	100	160	76.9	76.9	76.9	23.1	23.1
0.45	322	544	110	150	76.9	74.5	78.4	21.6	25.5
0.5	304	568	128	126	77.4	70.4	81.8	18.2	29.6
0.55	278	593	154	101	77.4	64.4	85.4	14.6	35.6
0.6	255	614	177	80	77.2	59.0	88.5	11.5	41.0
0.65	229	632	203	62	76.5	53.0	91.1	8.9	47.0
0.7	183	647	249	47	73.7	42.4	93.2	6.8	57.6
0.75	124	669	308	25	70.4	28.7	96.4	3.6	71.3
0.8	62	680	370	14	65.9	14.4	98.0	2.0	85.6
0.85	34	688	398	6	64.1	7.9	99.1	0.9	92.1
0.9	5	694	427	0	62.1	1.2	100.0	0.0	98.8
0.95	0	694	432	0	61.6	0.0	100.0	0.0	100.0
1	0	694	432	0	61.6	0.0	100.0	0.0	100.0